



# Probabilistic maximization of time-dependent capacities in a gas network

Holger Heitsch<sup>1</sup> · René Henrion<sup>1</sup> · Caren Tischendorf<sup>2</sup>

Received: 26 January 2024 / Revised: 5 July 2024 / Accepted: 10 July 2024 /  
Published online: 6 August 2024  
© The Author(s) 2024

## Abstract

The determination of free technical capacities belongs to the core tasks of a gas network owner. Since gas loads are uncertain by nature, it makes sense to understand this as a probabilistic problem provided that stochastic modeling of available historical data is possible. Future clients, however, do not have a history or they do not behave in a random way, as is the case, for instance, in gas reservoir management. Therefore, capacity maximization becomes an optimization problem with uncertainty-related constraints which are partially of probabilistic and partially of robust (worst case) type. While previous attempts to solve this problem were devoted to models with static (time-independent) gas flow, we aim at considering here transient gas flow subordinate to the isothermal Euler equations. The basic challenge addressed in the manuscript is two-fold: first, a proper way of formulating probabilistic constraints in terms of the differential equations has to be provided. This will be realized on the basis of the so-called spherical-radial decomposition of Gaussian random vectors. Second, a suitable characterization of the worst-case load behaviour of future customers has to be found. It will be shown, that this is possible for quasi-static flow and can be transferred to the transient case. The complexity of the problem forces us to constrain ourselves in this first analysis to simple pipes or to a V-like structure of the network. Numerical solutions are presented and show that the differences between quasi-static and transient solutions are small, at least in these elementary examples.

---

Dedicated to the memory of our teacher, colleague and friend Werner Römisch.

---

✉ Holger Heitsch  
holger.heitsch@wias-berlin.de  
René Henrion  
rene.henrion@wias-berlin.de  
Caren Tischendorf  
caren.tischendorf@hu-berlin.de

<sup>1</sup> Weierstrass Institute for Applied Analysis and Stochastics, Mohrenstraße 39, 10117 Berlin, Germany

<sup>2</sup> Institute of Mathematics, Humboldt-Universität zu Berlin, Unter den Linden 6, 10099 Berlin, Germany

**Keywords** Capacity maximization · Gas networks · Probabilistic constraints · Chance constraints · Transient flow

**Mathematics Subject Classification** 49M41 · 90B06 · 90C15

## 1 Introduction

This paper deals with the determination of time-dependent maximum free capacities in a gas network under uncertain loads. For a recent review on the transport capacity management of oil and gas pipeline networks we refer to Wang et al. (2022). The problem we are going to consider here is motivated by gas transport in an *entry-exit model* as it has been introduced, for instance, in Germany in 2005. In such a system, a *gas transmission system operator* (TSO) sells capacity rights (booking limits) to transport customers. These rights allow the customers to inject or withdraw gas up to the given capacity to entry or from exit points, respectively, in a completely independent manner under the condition that injections and withdrawals are in balance. The TSO has to make sure that the required gas transport can be technically realized for these arbitrary injections or withdrawals (nominations) within the given booking limits. Here, technical realization refers to the existence of pressure and flow functions satisfying the physical equations of gas transport such that the pressure in the pipes stays between given lower and upper bounds. He is obliged to offer a maximum possible capacity which can be used for booking, the so-called *freely allocable capacity* (FAC). On the other hand, the requirement to technically ensure the resulting gas transport for all possible nominations is not understood in a perfectly strict sense but for "likely and realistic" scenarios. For details of this model, we refer to the monograph (Koch et al. 2015, Chapters 3 and 14). The term "likely and realistic" already alludes to some probabilistic way of thinking: the concrete nominations vary from day to day depending on exterior conditions such as temperature. But even for given temperature there are random effects that make the consumption of gas stochastic.

It is clear that, in order to speak of a probability, one needs to have access to a statistical distribution of nominations. Such distributions are multivariate in character due to the presence of multiple nodes in the network but also due to time dependence. They can be estimated from historical gas load data available to TSOs as it is presented in (Koch et al. 2015 Chapter 13), where several types of multivariate distributions (e.g., Gaussian or log-normal) were found to be relevant for gas nomination data. However, contrary to gas load data of the existing clients at the exits, uncertainty in gas networks is not completely of stochastic nature. We list three such settings:

1. Gas injection at entries
2. Values of certain physical parameters
3. Gas load data of future clients which may benefit from FAC

As for 1., it has to be taken into account that the injection at different entry nodes is rather price-driven than random and could be output of a market model as in Grimm et al. (2017). Another approach to dealing with entry nominations is assuming a worst case with respect to technical realization of the required gas flow among all balanced

nominations as in Adelhütte et al. (2021) Chapter 2. To simplify this aspect, we shall assume in our paper, similar to (Gotzes et al. 2016; Heitsch 2020; Adelhütte et al. 2021 Chapter 3) that there is only a single entry node in the network feeding all the exit nodes so that the injection at the only entry is already determined by the total load of all exits and no uncertain splitting of this total load between several entries has to be considered.

Concerning 2., the most prominent unknown physical parameter is the roughness coefficient of a gas pipe. This value may differ in an unknown way from the original value after a possibly long time of aging and hardly be directly measured for pipes underground. Then, this value can be treated as an uncertain parameter in the sense of robust optimization (Aßmann et al. 2019) or it can be endowed with statistical information via uncertainty quantification and Markov chain Monte Carlo method (Heitsch and Strogies 2019). In this paper, we shall assume, all physical parameters to be known.

Most important for us is instance 3. While the gas load of existing clients maybe assumed to be stochastic thanks to historical data, the same is not true for future clients for which the FAC is potentially reserved. One could assume, for simplicity, that they will follow the same statistical characteristics as the existing clients, but this may not be justified for instance due to differing demographic factors. More importantly, FAC might be used, for instance, by the owner of a gas reservoir whose load profile is not random at all but might follow some optimization purposes which may be hard to predict. Then, the network owner has to be prepared for the worst case load profile within the booking limits offered to the new clients as an outcome of the determined FAC.

Therefore, the uncertain total demand of existing and potentially new clients (after exploiting FAC) exhibits a mixture of stochastic and worst case character. This leads to the formulation of a probabilistic-robust (proburst for short) constraint as introduced in González Grandón et al. (2017) in order to describe the technical feasibility of the determined FAC. In words, the optimization problem we want to solve is the following:

*Maximize FAC such that at least with a given probability the sum of random loads imposed by existing clients and arbitrary loads of up to the value of FAC imposed by future clients can be technically satisfied.*

We shall refer to this problem as the *probabilistic capacity maximization problem*. Note that FAC may be different from one exit node to the other, so maximizing might refer to the sum of node-dependent FACs or similar norms. In Heitsch (2020), the probabilistic capacity maximization problem has been investigated without time-dependence for an algebraic model of stationary gas flow respecting mass balance, pressure drop and pressure bounds at the (single) entry and the exits. However, gas loads at the exits may strongly vary over time in the course of a day which also has a temporal impact on the free capacity FAC. We therefore intend to study here a probabilistic maximization of time-dependent capacities implied by time-dependent loads. We shall investigate whether the time dependence of gas flow can be assumed to be quasi-static, which drastically simplifies the model and, in particular, the probabilistic treatment of technical feasibility or a PDE-based transient model has to be employed. As stated in Gugat et al. (2023), for demand functions that change very slowly in time, it makes sense to consider a quasi-static model, since at each moment the system state

is very close to a steady state. In order to get realistic results, we model time-dependent stochastic demands of existing clients based on historical data.

Mathematically, the problem formulated above verbally will lead to a so-called *probabilistic constraint* embedded into a possibly PDE-constrained optimization problem. We note that probabilistic constraints in the context of control problems with transient gas flow have also been investigated in several other works such as (Adelhütte et al. 2021; Göttlich et al. 2021; Schuster et al. 2022). The present paper differs from these first of all in the concrete problem of maximizing time-dependent free capacities but also in the numerical treatment of probabilistic constraints (spherical-radial decomposition adapted to the discretization of the underlying PDE). As mentioned above, a major challenge in our model is the integration of non-stochastic loads by future clients into the probabilistic constraints. Formally, one would have to admit arbitrary load-functions here, which is out of reach in an optimization context. Fortunately, in a quasi-static model, the worst-case load profile of a new client, given a scenario for the stochastic load of an existing client can be explicitly verified. The idea then is, to keep this information and use it as a constraint in a PDE-based model as an approximate substitute for a general, unknown worst case.

The paper is organized as follows: In Sect. 2, which is devoted to a single pipe, we introduce first the concept of technical feasibility for transient and quasi-static gas flow. Then, taking into account random loads of existing clients and completely uncertain (non-stochastic) loads of future clients, the capacity maximization problem is presented along with an appropriate probabilistic constraint involving additional robust constraints inside. After describing the discretization of the PDE - which leads to two coupled ODEs - a statistical model for historical gas load patterns is presented. Finally, it is demonstrated, how the *spherical radial decomposition* of Gaussian random vectors can be employed to numerically deal with the probabilistic constraint in the environment of ODEs with random coefficients. Section 3 demonstrates, how one can make the probabilistic constraint explicit in the case of quasi-static gas flow by identifying the worst-case behaviour of future clients. This identification is then taken as a basis for the case of transient gas flow too. A numerical comparison between both transport models is provided. Section 4 generalizes the previous ideas conceptually from the consideration of a single pipe to a network with tree structure. Numerical results are presented for a simple V-shaped form of the network.

## 2 Probabilistic capacity maximization on a single pipe

In order to illustrate the main ideas of our approach and to keep the notation simple, we start considering the problem of probabilistic capacity maximization for a single pipe whose left end is an entry at which gas is injected whereas the right end corresponds to an exit, where gas is withdrawn to meet a certain (random) demand.

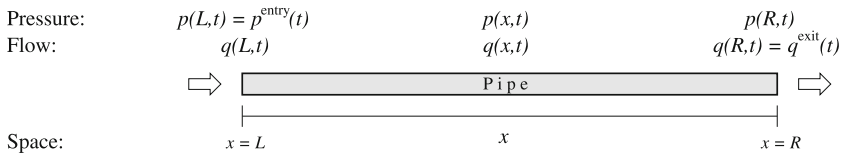


Fig. 1 Illustration of the introduced notation for a single pipe

### 2.1 Transient and quasi-static transport models for a single pipe

An overview of different models for the description of gas flow in gas networks is provided by Domschke et al. (2021). In the following we consider the gas flow through a single pipe and make use of the following notation:

- $a_s$  ... speed of sound (unit  $[m\ s^{-1}]$ ),
- $A$  ... the cross section (unit  $[m^2]$ ),
- $D$  ... the diameter of the pipe (unit  $[m]$ ),
- $\lambda$  ... the friction coefficient of the pipe (scalar),
- $h$  ... length of the pipe (unit  $[m]$ ).

We consider the *isothermal Euler equations* for gas pressure  $p(x, t)$  (unit  $[kg\ m^{-1}s^{-2}]$ ) and gas flow  $q(x, t)$  (unit  $[kg\ s^{-1}]$ ) during a time horizon  $[0, T]$  along a pipe  $[L, R]$ , where the left end  $L$  will be identified with an entry where gas is injected and the right end  $R$  with an exit where gas is consumed:

$$\begin{aligned} \partial_t p + \alpha \partial_x q &= 0 \\ \partial_t q + \beta \partial_x p + \gamma \frac{q|q|}{p} &= 0 \end{aligned} \quad (x, t) \in [L, R] \times [0, T] \tag{1}$$

with constants

$$\alpha := \frac{a_s^2}{A}, \quad \beta := A, \quad \gamma := \frac{\lambda a_s^2}{2DA}.$$

The Eq. (1) have to be augmented by initial and boundary conditions:

$$\begin{aligned} p(L, t) &= p^{\text{entry}}(t); \quad q(R, t) = q^{\text{exit}}(t) \quad \forall t \in [0, T] \\ \text{and } p(R, 0) &= p_R^0; \quad q(L, 0) = q_L^0. \end{aligned} \tag{2}$$

An illustration of the introduced notation is given in Fig. 1.

In the following sections,  $q^{\text{exit}}$  will be modeled as a stochastic process based on historical data. The pressure at the entry  $p^{\text{entry}}$  is not given but is looked for within the optimization problem. This will become clearer from the following definition.

**Definition 1** A load profile  $q^{\text{exit}}$  for gas withdrawal at the exit will be said to be technically feasible w.r.t. **transient** gas flow if there exists a pressure profile  $p^{\text{entry}}$  at

the entry and a solution  $(p, q)$  of the PDE (1) satisfying boundary and initial conditions (2) and the constraints

$$p^{\text{entry}}(t) \in [p_{\text{entry}}^{\min}, p_{\text{entry}}^{\max}]; \quad p(R, t) \in [p_R^{\min}, p_R^{\max}] \quad \forall t \in [0, T], \quad (3)$$

where  $p_{\text{entry}}^{\min} \leq p_{\text{entry}}^{\max}$  and  $p_R^{\min} \leq p_R^{\max}$  are given lower and upper pressure bounds at the entry and exit, respectively.

The model drastically simplifies when assuming stationary gas flow, in which case pressure and flow are constant in time (and as a consequence, flow is also constant in space) and are related by the so-called *Weymouth equation*:

$$p^2(L) - p^2(x) = 2(x - L) \frac{\gamma}{\beta} q|q| \quad (x \in [L, R]). \quad (4)$$

The stationary case is not relevant by itself for our purposes, because we will deal with time-dependent exit loads. However, the so-called *quasi-static* case will be of much interest. Here, it is assumed that the system is in steady state at each moment in time. Then, the time-dependent version of the steady state relation (4) becomes

$$p^2(L, t) - p^2(x, t) = 2(x - L) \frac{\gamma}{\beta} q(t)|q(t)| \quad (x \in [L, R], t \in [0, T]).$$

Reducing this to  $x = R$ , which is essential in the pressure bound relations (3), taking into account the boundary conditions (2), and identifying the space-independent flow  $q$  with  $q^{\text{exit}}$ , one ends up at

$$(p^{\text{entry}}(t))^2 - p^2(R, t) = \tilde{\gamma} q^{\text{exit}}(t)|q^{\text{exit}}(t)| \quad (t \in [0, T]) \quad \text{with} \quad \tilde{\gamma} := 2h \frac{\gamma}{\beta}. \quad (5)$$

Accordingly, we are led to the following definition.

**Definition 2** A load profile  $q^{\text{exit}}$  for gas withdrawal at the exit will be said to be technically feasible w.r.t. **quasi-static** gas flow if there exist pressure profiles  $p^{\text{entry}}, p(R, \cdot)$  at the entry and exit, respectively, satisfying (5) and the constraints (3).

### 2.2 The optimization problem with implicit probabilistic constraint

We now want to formalize in the case of a single pipe the probabilistic capacity maximization problem presented verbally in the introduction. To this aim, we introduce the sets

$$\begin{aligned} \mathcal{T}^{\text{trans}} &:= \{ q^{\text{exit}}(\cdot) \mid q^{\text{exit}} \text{ is technically feasible w.r.t. transient gas flow} \} \\ \mathcal{T}^{\text{qstat}} &:= \{ q^{\text{exit}}(\cdot) \mid q^{\text{exit}} \text{ is technically feasible w.r.t. quasi-static gas flow} \} \end{aligned}$$

of technically feasible load profiles at the exit according to Definitions 1 and 2. We shall assume that the time-dependent free capacity FAC we are aiming to maximize is

offered as a constant for each of the  $T = 24$  h of a day. On the one hand, this appears to be more practical in a real-life implementation than capacities which are continuous in time. On the other hand, we get already a canonical discretization of the control function as a finite-dimensional vector. Now, the probabilistic capacity maximization problem for transient or quasi-static gas flow, respectively, can be stated as follows:

$$\max_{(u_1, \dots, u_{24}) \in \mathbb{R}_+^{24}} \left\{ \sum_{i=1}^{24} u_i \mid \mathbb{P} \left( \xi + y \in \mathcal{T}^{\text{trans/qstat}} \text{ for all } y : [0, T] \rightarrow \mathbb{R} \right. \right. \tag{6}$$

$$\left. \left. \text{such that } 0 \leq y \leq U := \sum_{i=1}^{24} u_i \chi_{(i-1, i]} \right) \geq p \right\}.$$

Here,  $U$  refers to the time-dependent free capacity FAC which is assumed to be in hourly discretization. Hence, it is defined by the vector  $(u_1, \dots, u_{24})$  and by characteristic functions  $\chi_{(i-1, i]}$  taking value one if the argument belongs to the interval  $(i - 1, i]$  and zero otherwise). For notational simplicity the sum of them, formally defined on  $(0, T]$  only, is understood as function on  $[0, T]$  with value  $u_1$  at argument 0). The load profile at the exit is supposed to be the sum  $q^{\text{exit}} = \xi + y$  of the load  $\xi$  of existing clients, modeled as a stochastic process whose statistical characteristics are supposed to be known from historical data, and of the load  $y$  of potentially new clients to which the free capacity  $u$  is allocated. For the latter nothing is known apart from the fact that these loads must be in between 0 and  $u_i$  at each hour  $i$ . The threshold  $p \in (0, 1]$  is a pre-defined probability level at which the probabilistic constraint inside (6) is required to hold. More precisely, this constraint expresses the fact that, given a profile  $u$  of time-dependent FAC, the probability  $\mathbb{P}$  of a total exit load composed from existing clients (acting randomly) and potential new clients (acting unpredictably, hence, arbitrarily) being technically feasible exceeds a given value  $p$ .

We already note at this point, that the form of the probabilistic constraint in (6) is implicit and does not correspond yet to the standard form involving a random inequality system as presented in Sect. 2.5 below.

### 2.3 Discretization of the PDE

For the numerical treatment of transient gas flow along a pipe according to (1), we follow (Huck and Tischendorf 2017) and use a two-point space discretization (left and right end of the pipe) and (exemplarily) an implicit Euler discretization with respect to time. Modern discretization schemes are based on a port-Hamiltonian formulation of the pipe network system. They combine mixed finite element approximations in space with an implicit time stepping scheme and ensure the global conservation of mass and energy, see e.g. Egger (2018); Egger et al. (2023).

We assume that the time interval  $[0, T]$  is uniformly discretized in  $N$  subintervals of length  $\tau = T/N$ . The discretization scheme for the pressure  $p = p(R, \cdot)$  at the right end and the flow  $q = q(L, \cdot)$  at the left end of the pipe is then given by

$$\begin{aligned}
 p^k &:= p^{k-1} - a(z^k - q^k) \\
 q^k &:= q^{k-1} + b(w^k - p^k) - c \frac{(q^k)^2}{p^k} \quad (k = 1, \dots, N)
 \end{aligned}
 \tag{7}$$

with coefficients calculated from those introduced in (1) as

$$a := \tau \frac{\alpha}{h}; \quad b := \tau \frac{\beta}{h}; \quad c := \tau \gamma.$$

Here,  $w^k := p^{\text{entry}}(k\tau) = p(L, k\tau)$  is the time-dependent pressure profile at the entry (left end of the pipe) and  $z^k := q^{\text{exit}}(k\tau) = q(R, k\tau)$  is the (random) load profile at the exit(right end of the pipe). As far as the initial conditions  $p^0 := p_R^0$  and  $q^0 := q_L^0$  are concerned, they are not known in general, in particular not for the historical load profiles used in Sect. 2.4 for the statistical modeling of gas load data. A common remedy is to fall back on the stationary case (see 4) and to suppose that

$$q^0 = z^0 = q^{\text{exit}}(0); \quad p^0 = \sqrt{(p^{\text{entry}}(0))^2 - \tilde{\gamma} q^{\text{exit}}(0) |q^{\text{exit}}(0)|}.$$

In any case, the dependence of the transient state on the concrete initial value can be observed only on a very short time scale so that we will neglect it in the following. More precisely, we shall fix a common 'average' value for  $p_R^0, q_L^0$  and disregard any relation with or dependence on a concrete random load scenario at the exit.

In order to find  $(p^k, q^k)$  from the implicit system (7), we solve the first linear relation for  $q^k$  and then insert it into the second relation. This yields a quadratic expression in terms of  $p^k$  which is resolved as

$$p^k = \frac{1}{r} \left( \frac{u}{2} + \sqrt{\frac{u^2}{4} + rv} \right) \quad \text{and} \quad q^k = \frac{p^k - p^{k-1}}{a} + z^k,$$

where the numbers  $r, u, v$  are given by

$$\begin{aligned}
 r &:= a^2 b + a + c \\
 u &:= a^2 (bw^k + q^{k-1} - z^k) + a (p^{k-1} - 2cz^k) + 2cp^{k-1} \\
 v &:= c (2ap^{k-1}z^k - (p^{k-1})^2 - a^2(z^k)^2).
 \end{aligned}$$

In our application it will be important also to keep track of the dependence of state variables  $p, q$  on an exterior parameter  $e$  which will be mainly be represented by the random variable and by the decision (control) variable. Therefore, we derive an analogous iteration scheme for the gradients of  $p^k$  and  $q^k$  with respect to  $e$  by differentiation of (7):



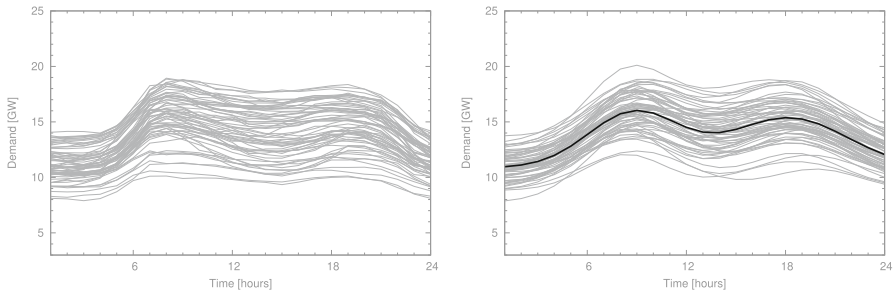


**Fig. 2** Plot of historical gas load scenarios (left) and simulated scenarios from the estimated statistical distribution (right, thick: mean value  $\mu$ )

$$\begin{aligned} \nabla p^k &:= \nabla p^{k-1} - a \left( \nabla z^k - \nabla q^k \right) \\ \nabla q^k &:= \nabla q^{k-1} - b \left( \nabla w^k - \nabla p^k \right) - c \frac{2p^k q^k \nabla q^k - (q^k)^2 \nabla p^k}{(p^k)^2} \quad (k = 1, \dots, N) \end{aligned}$$

for given initial gradients  $\nabla p^0$  and  $\nabla q^0$ . This represents a linear system of equations that, along with the solutions  $p^k, q^k$  from above, is solved by:

$$\begin{aligned} \nabla p^k &= \frac{((p^k)^2 + 2cp^k q^k) (a\nabla z^k - \nabla p^{k-1}) - a(p^k)^2(\nabla q^{k-1} + b\nabla w^k)}{ac(q^k)^2 - (ab + 1)(p^k)^2 - 2cp^k q^k} \\ \nabla q^k &= \frac{\nabla p^k - \nabla p^{k-1}}{a} + \nabla z^k \end{aligned} \tag{8}$$

We note that the described scheme can be extended to a finer space discretization if needed, for instance by adding the mean point of the pipe in order to get a three-point discretization scheme.

### 2.4 Statistical model for gas load patterns

The treatment of the probabilistic constraint in our optimization problem(s) (6) requires to represent the stochastic process  $\xi$  in a parametric form. More precisely, we shall assume a functional dependence  $\xi(t) = d(\tilde{\xi}, t)$  for all  $t \in [0, T]$  where  $\tilde{\xi}$  is some finite dimensional random vector. In order to get a realistic statistical model of daily gas load profiles, we considered publicly available hourly load data from Austria ([EnergyMonitor.at](http://EnergyMonitor.at)). More precisely, the corresponding data were drawn from week days (in order to disregard different patterns on weekends) in the three winter months (in order to disregard seasonal trends) from December 2013 to February 2014. This resulted in 65 historical scenarios for 24 h each. They are plotted in Fig. 2 (left).

It can be seen that the daily gas load typically exhibits two peaks in the morning and in the afternoon, but the position, amplitudes and band widths of these peaks vary in different scenarios. This leads us to formulate a statistical model for the gas load as

$$d(\tilde{\xi}_1, \dots, \tilde{\xi}_7, t) = \tilde{\xi}_1 + \tilde{\xi}_2 e^{-e^{\tilde{\xi}_3} (t - \tilde{\xi}_4)^2} + \tilde{\xi}_5 e^{-e^{\tilde{\xi}_6} (t - \tilde{\xi}_7)^2} \quad t \in [0, T], \tag{9}$$

where the random coefficients  $\tilde{\xi}_i$  model the shapes of the two peaks for  $i = 2, \dots, 7$  and  $\tilde{\xi}_1$  represents some base line for the load. We assume that the joint distribution of the random vector  $\tilde{\xi}$  is Gaussian according to  $\tilde{\xi} \sim \mathcal{N}(\mu, \Sigma)$  with mean vector  $\mu$  and covariance matrix  $\Sigma$ . This means, in particular, that the coefficients  $e^{\tilde{\xi}_3}, e^{\tilde{\xi}_6}$  modeling the band widths of the peaks are supposed to represent log-normal coefficients. The parameters  $\mu$  and  $\Sigma$  were found from a statistical fit to the historical data using the MATLAB built-in function `nlinfit`. More precisely, the concrete parameters

$$\mu = (10.8679, 5.0149, -2.7452, 8.8464, 4.4975, -3.2350, 18.1880)$$

and

$$\Sigma = \begin{pmatrix} 1.5467 & 0.0350 & 0.0049 & 0.0915 & 0.1119 & 0.0037 & -0.2588 \\ 0.0350 & 0.7836 & -0.0309 & 0.0084 & 0.8738 & -0.0940 & -0.0553 \\ 0.0049 & -0.0309 & 0.0646 & -0.0598 & 0.0012 & -0.0443 & -0.0712 \\ 0.0915 & 0.0084 & -0.0598 & 0.1205 & 0.0251 & 0.0397 & 0.0486 \\ 0.1119 & 0.8738 & 0.0012 & 0.0251 & 1.3963 & -0.2593 & -0.3194 \\ 0.0037 & -0.0940 & -0.0443 & 0.0397 & -0.2593 & 0.1280 & 0.1640 \\ -0.2588 & -0.0553 & -0.0712 & 0.0486 & -0.3194 & 0.1640 & 0.3888 \end{pmatrix}$$

have been determined. Of course, these data representing gas loads of a big region will not be used directly in our numerical computations for a single pipe. Rather, they will be downscaled by an appropriate factor. This means that we replace  $d$  in (9) by  $s \cdot d$  for some  $s > 0$  while keeping the derived statistical distribution for the random vector.

### 2.5 Spherical-radial decomposition of Gaussian random vectors

Probabilistic constraints are constraints on a decision variable  $u$  which is affected by some finite-dimensional random vector  $\eta$  inside an inequality system describing the constraint of an optimization problem. More precisely, one requires that, given  $u$ , this random inequality system be satisfied with some minimum probability  $p \in (0, 1]$ :

$$\mathbb{P}(g_k(u, \eta) \leq 0 \quad (k = 1, \dots, M)) \geq p. \tag{10}$$

Here, we assume that the functions  $g_k$  are continuously differentiable. Introduced in the fifties by Charnes, Cooper and Symonds (Charnes et al. 1958), the basics of probabilistic constraints have been intensively investigated starting with the seventies and the fundamental work by Prékopa. Still today, his later monograph is a classical reference for this domain (Prékopa 1995). For more recent presentations we refer to van Ackooij (2020); Shapiro et al. (2009). The algorithmic treatment of probabilistic constraints has seen a fresh impetus during the last two decades (see e.g., van Ackooij et al. (2021); Berthold et al. (2022); Curtis et al. (2018); Geletu et al.

(2020); Keil et al. (2021); Luedtke and Ahmed (2008); Pagnoncelli et al. (2009) for a very incomplete selection). We shall make use in this work of the so-called *spherical-radial decomposition* of Gaussian random vectors which has been successfully applied to numerous optimization problems with probabilistic constraints (e.g., Berthold et al. (2022); Farshbaf-Shaker et al. (2020); González Grandón et al. (2017); Heitsch (2020)). The advantage of this approach over methods relying on generic sampling of an arbitrary distribution consists in exploiting specific information about the Gaussian distribution which yields a significant variance reduction in the estimation of probabilities.

In this section we show how to approximate efficiently values and gradients of a probability function

$$\varphi(u) := \mathbb{P}(g_k(u, \eta) \leq 0 \quad (k = 1, \dots, M)) \tag{11}$$

with  $u \in \mathbb{R}^n$  and  $\eta \sim \mathcal{N}(\mu, \Sigma)$  being an  $m$ -dimensional Gaussian random vector with expectation  $\mu$  and covariance matrix  $\Sigma$ . This will be the key for dealing with the inequality constraint  $\varphi(u) \geq p$  (corresponding to 10) inside a nonlinear optimization solver, say some SQP method. The principle of spherical-radial decomposition of the Gaussian random vector  $\eta$  expresses the fact that, for every Borel measurable subset  $C \subseteq \mathbb{R}^m$  one has the representation

$$\mathbb{P}(\eta \in C) = \int_{w \in \mathbb{S}^{m-1}} \nu_{\text{chi}}(\{r \geq 0 \mid \mu + rLw \in C\}) \, dv_u(w),$$

where  $\mathbb{S}^{m-1}$  is the unit sphere in  $\mathbb{R}^m$ ,  $\nu_{\text{chi}}$  is the one-dimensional Chi-distribution with  $m$  degrees of freedom,  $v_u$  is the uniform distribution on  $\mathbb{S}^{m-1}$  and the matrix  $L$  of order  $(m, m)$  is a root of  $\Sigma$  (i.e.,  $\Sigma = LL^T$ ). Applied to (11), this yields the expression

$$\varphi(u) = \int_{w \in \mathbb{S}^{m-1}} \nu_{\text{chi}}(\{r \geq 0 \mid g_k(u, \mu + rLw) \leq 0 \quad (k = 1, \dots, M)\}) \, dv_u(w). \tag{12}$$

Generically, the one-dimensional set whose Chi-probability has to be computed in the integrand above can be represented as a finite union of disjoint intervals

$$\bigcup_{j=1}^{N(u,w)} [\alpha_j(u, w), \beta_j(u, w)]$$

which depend on both, the argument  $u$  and the direction  $w$ . Note, that this set could be unbounded in which case  $\beta_{N(u,w)} = \infty$  (while always  $\alpha_1(u, w) \geq 0$ ). As a consequence,

$$\varphi(u) = \int_{w \in \mathbb{S}^{m-1}} \sum_{j=1}^{N(u,w)} (F_{\text{chi}}(\beta_j(u, w)) - F_{\text{chi}}(\alpha_j(u, w))) \, dv_u(w),$$

where  $F_{\text{chi}}$  refers to the cumulative distribution function of the one-dimensional Chi-distribution with  $m$  degrees of freedom. For a numeric approximation of  $\varphi(u)$ , one would replace the spherical integral by a finite sum with respect to a sample  $\{w^1, \dots, w^K\}$  of the uniform distribution on the sphere  $\mathbb{S}^{m-1}$ :

$$\varphi(u) \approx \frac{1}{K} \sum_{l=1}^K \sum_{j=1}^{N(u, w^l)} \left( F_{\text{chi}}(\beta_j(u, w^l)) - F_{\text{chi}}(\alpha_j(u, w^l)) \right). \tag{13}$$

An efficient sample could be provided by a low discrepancy sequence on the sphere. A simple alternative is a QMC sample of the  $m$ -dimensional standard Gaussian distribution normalized to unit length. We note that numerically precise approximations of  $F_{\text{chi}}$  are part of standard statistical modules. Hence, the main effort in the approximation of  $\varphi(u)$  consists in the determination of the coefficients  $\alpha_j, \beta_j$ . This is an easy task in case that the functions  $g_k(u, \eta)$  are linear or quadratic in  $\eta$  (the quadratic case occurs, for instance, in the random inequality system derived for the quasi-static model in Sect. 3.1). Otherwise, an analytic derivation of these coefficients may become impossible and has to be replaced by some one-dimensional root finding or a bisection approach. This will be the case in our application because the nonlinearities arising from the statistical gas load model (9) as well as from the discretized PDE in Sect. 2.3 are too complex.

In addition to evaluating the probability function  $\varphi$  itself, an efficient numerical treatment of the optimization problem (e.g., using SQP methods) will also require its gradient  $\nabla\varphi$ . If we look for instance at (13), then an approximation of the gradient can be obtained as

$$\nabla\varphi(u) \approx \frac{1}{K} \sum_{l=1}^K \sum_{j=1}^{N(u, w^l)} \left( \frac{\partial(F_{\text{chi}} \circ \beta_j)}{\partial u}(u, w^l) - \frac{\partial(F_{\text{chi}} \circ \alpha_j)}{\partial u}(u, w^l) \right). \tag{14}$$

Given that  $F'_{\text{chi}} = f_{\text{chi}}$  with  $f_{\text{chi}}$  being the density of the one-dimensional Chi-distribution with  $m$  degrees of freedom, we obtain for  $j = 1, \dots, N(u, w^l)$  and  $l = 1, \dots, K$  that

$$\frac{\partial(F_{\text{chi}} \circ \beta_j)}{\partial u}(u, w^l) = f_{\text{chi}}(\beta_j(u, w^l)) \cdot \frac{\partial\beta_j}{\partial u}(u, w^l)$$

(the analogous expression holding true for  $\alpha_j$ ). Observing that the coefficients,  $\alpha_j, \beta_j$  are values of  $r$  in (12) for which one of the inequalities  $g_k(u, \mu + rLw) \leq 0$  is satisfied as an equality, one may apply the Implicit Function Theorem to that equality in order to obtain the derivatives

$$\frac{\partial\beta_j}{\partial u}(u, w^k) = \frac{-1}{\langle \nabla_{\eta} g_{k^*}(u, \mu + \beta_j(u, w^l)Lw^l), Lw^l \rangle} \nabla_u g_{k^*}(u, \mu + \beta_j(u, w^l)Lw^l),$$

where  $k^* \in \operatorname{argmax} \{g_k(u, \mu + \beta_j(u, w^l)Lw^l) \mid k \in \{1, \dots, M\}\}$ . The analogous expression holds true for the coefficients  $\alpha_j$ . In this way, a fully explicit representation

of the approximated  $\nabla\varphi(u)$  may be provided which just involves the initial data (partial derivatives of the functions  $g_k$ ) of the problem. Observe, that the sample-dependent coefficients  $\alpha_j, \beta_j$  needed for the gradient  $\nabla\varphi$  are the same already needed for the probability function  $\varphi$  itself. Hence, one may update  $\varphi$  and  $\nabla\varphi$  simultaneously with the same sample and the computational effort in determining  $\alpha_j, \beta_j$  occurs only once.

We note that the application of the Implicit Function Theorem mentioned above requires justification which may be rigorously possible in certain special cases (e.g., the quasi-static flow discussed in Sect. 3.1) but could be difficult in general (e.g., the transient flow discussed in Sect. 3.4). For a detailed discussion of this issue we refer to van Ackooij (2020) and papers cited therein.

### 3 Explicit probabilistic constraints for a single pipe

As already stated above, the probabilistic constraint in our capacity maximization problem (6) is not explicit yet and thus not directly amenable to a numerical solution via some optimization solver. The reason is that first, the definition of technical feasibility, hence the definition of the sets  $\mathcal{T}^{\text{trans/qstat}}$  asks for the existence of some pressure profile  $p^{\text{entry}}$  satisfying certain properties. One could resolve this issue by understanding  $p^{\text{entry}}$  as an additional decision variable in the optimization problem (6). Then, however, the solution of the capacity maximization problem would not only fix the free capacities but also the pressure profile at which gas is injected at the entry, independently of the concrete load scenarios. Such an approach would drastically decrease the free capacities one could actually allocate. Understanding  $p^{\text{entry}}$  as a function of loads instead would lead to the question of how to find this function. It would be optimal to determine it in a way as to maximize the probability of satisfying the pressure bounds (3). This, however, seems to be a hopeless task in the given context. A second, even more important difficulty in the definition of technical feasibility, relies on the arbitrary choice of loads  $y$  from new customers within the limits of free capacity in (6). This ambiguity makes it basically impossible to deal with the probabilistic constraint as is in the context of an optimization algorithm. Fortunately, as we shall see, these issues can be resolved in the quasi-static model by equivalently describing the relation inside the probability in (6) as an explicit inequality system involving only the random parameter  $\xi$  and the decision variable  $u$  but no more the undetermined variables  $p^{\text{entry}}$  and  $y$ . Therefore, our proposal for the transient model is to adapt from the quasi-static model the way of making the probability explicit while keeping the description of dynamics via the PDE (1).

#### 3.1 The quasi-static case

The aim of this section is to provide an equivalent description of the implicit probabilistic constraint inside (6) in an explicit standard form involving only the random and the decision variable as assumed in Sect. 2.5.

**Proposition 1** For a given exit load profile  $q^{\text{exit}} \geq 0$  the following equivalence holds true:

$$q^{\text{exit}} \in \mathcal{T}^{\text{qstat}} \iff \left( p_{\text{entry}}^{\min} \right)^2 - \left( p_R^{\max} \right)^2 \leq \tilde{\gamma}(q^{\text{exit}}(t))^2 \leq \left( p_{\text{entry}}^{\max} \right)^2 - \left( p_R^{\min} \right)^2 \quad \forall t \in [0, T]. \tag{15}$$

**Proof** ( $\implies$ ): Let  $q^{\text{exit}} \geq 0$  with  $q^{\text{exit}} \in \mathcal{T}^{\text{qstat}}$  be arbitrarily given. Then, by definition of  $\mathcal{T}^{\text{qstat}}$ , there exist pressure profiles  $p^{\text{entry}}, p(R, \cdot)$  satisfying the relations (5) and (3). Taking into account that  $q^{\text{exit}} \geq 0$  and substituting for  $p_R$  in (5), the (squared) second pressure bound relations in (3) read as

$$\left( p_R^{\min} \right)^2 \leq \left( p^{\text{entry}}(t) \right)^2 - \tilde{\gamma}(q^{\text{exit}}(t))^2 \leq \left( p_R^{\max} \right)^2 \quad \forall t \in [0, T].$$

Using the (squared) first pressure bound relations in (3), we may continue to estimate these relations in order to derive the right-hand side relations of the asserted equivalence (15).

( $\impliedby$ ): Let  $q^{\text{exit}} \geq 0$  be given such that the the right-hand side inequalities of (15) are satisfied. Define, for  $t \in [0, T]$ ,

$$p^{\text{entry}}(t) := \min \left\{ p_{\text{entry}}^{\max}, \sqrt{\tilde{\gamma}(q^{\text{exit}}(t))^2 + \left( p_R^{\max} \right)^2} \right\}, \tag{16}$$

$$p(R, t) := \sqrt{\left( p^{\text{entry}}(t) \right)^2 - \tilde{\gamma}(q^{\text{exit}}(t))^2}.$$

Then, by definition,  $p^{\text{entry}}, p(R, \cdot)$  satisfy (5) and it holds that  $p^{\text{entry}}(t) \leq p_{\text{entry}}^{\max}$ . Moreover,  $p^{\text{entry}}(t) \geq p_{\text{entry}}^{\min}$  thanks to the first inequality on the right-hand side of (15). Hence, the pressure bound conditions for  $p^{\text{entry}}(t)$  in (3) are fulfilled. Finally, for each  $t \in [0, T]$ ,

$$p(R, t) = \begin{cases} \sqrt{\left( p_{\text{entry}}^{\max} \right)^2 - \tilde{\gamma}(q^{\text{exit}}(t))^2} & \text{if } p_{\text{entry}}^{\max} \leq \sqrt{\tilde{\gamma}(q^{\text{exit}}(t))^2 + \left( p_R^{\max} \right)^2} \\ p_R^{\max} & \text{else} \end{cases}.$$

In the second case, the pressure bound conditions for  $p(R, t)$  in (3) are trivially satisfied. In the first case,  $p(R, t) \geq p_R^{\min}$  thanks to the second inequality on the right-hand side of (15). Combining the inequality which defines the first case with the formula for  $p(R, t)$  arising in that case yields the missing relation  $p(R, t) \leq p_R^{\max}$ . Summarizing,  $q^{\text{exit}} \in \mathcal{T}^{\text{qstat}}$ .  $\square$

**Corollary 1** For a given exit load profile  $q^{\text{exit}} \geq 0$  and a given profile  $U \geq 0$  of time-dependent free capacities the following equivalence holds true:

$$q^{\text{exit}} + y \in \mathcal{T}^{\text{qstat}} \quad \forall y : [0, T] \rightarrow \mathbb{R} : 0 \leq y \leq U$$

$$\iff$$

$$\begin{aligned} & \left(p_{\text{entry}}^{\min}\right)^2 - \left(p_R^{\max}\right)^2 \leq \tilde{\gamma}(q^{\text{exit}}(t))^2 \text{ and} \\ & \tilde{\gamma}\left(q^{\text{exit}}(t) + U(t)\right)^2 \leq \left(p_{\text{entry}}^{\max}\right)^2 - \left(p_R^{\min}\right)^2 \quad \forall t \in [0, T] \end{aligned} \tag{17}$$

**Proof** Replacing  $q^{\text{exit}}$  in Proposition 1 by  $q^{\text{exit}} + y$ , we observe that the left part of our asserted equivalence (17) is equivalent with the relation

$$\left(p_{\text{entry}}^{\min}\right)^2 - \left(p_R^{\max}\right)^2 \leq \tilde{\gamma}\left(q^{\text{exit}}(t) + y(t)\right)^2 \leq \left(p_{\text{entry}}^{\max}\right)^2 - \left(p_R^{\min}\right)^2 \quad \forall t \in [0, T]$$

holding true for all  $y : [0, T] \rightarrow \mathbb{R} : 0 \leq y \leq U$ . Now, fixing an arbitrary  $t \in [0, T]$ , it is clear from  $y(t) \geq 0$  that the first inequality will be satisfied for all indicated functions  $y$  if and only if it is satisfied for  $y:=0$ . Likewise, it follows from  $y(t) \leq U(t)$  that the second inequality will be satisfied for all indicated functions  $y$  if and only if it is satisfied for  $y:=U$ . This yields the equivalence with the relations in the right part of (17). □

According to Corollary 1, the relation

$$\xi + y \in \mathcal{T}^{\text{qstat}} \quad \forall y : [0, T] \rightarrow \mathbb{R} : 0 \leq y \leq U$$

for a random exit load profile  $\xi$  and some time-dependent function  $U$  of free capacities can be equivalently described by the inequalities

$$h_i(u, \xi, t) \leq 0 \quad \forall t \in [0, T] \quad (i = 1, 2),$$

where, for  $t \in [0, T]$ ,

$$\begin{aligned} h_1(U, \xi, t) & := \left(p_{\text{entry}}^{\min}\right)^2 - \left(p_R^{\max}\right)^2 - \tilde{\gamma}\xi^2(t), \\ h_2(U, \xi, t) & := \tilde{\gamma}\left(\xi(t) + U(t)\right)^2 - \left(p_{\text{entry}}^{\max}\right)^2 + \left(p_R^{\min}\right)^2. \end{aligned}$$

We now take into account (1) our statistical model (9), (2) the time discretization of pressure and flow variables into  $N$  subintervals of  $[0, T]$  of equal length with  $T = 24$  and (3) the hourly discretization of the free capacities in (6). Then, the inequalities above turn into the finite random inequality system  $g_\ell(u, \tilde{\xi}) \leq 0$  for  $\ell = 1, \dots, 2N$ ; where for  $k = 1, \dots, N$

$$\begin{aligned} g_k(u, \tilde{\xi}) & := \left(p_{\text{entry}}^{\min}\right)^2 - \left(p_R^{\max}\right)^2 - \tilde{\gamma}d^2(\tilde{\xi}, t_k), \\ g_{N+k}(u, \tilde{\xi}) & := \tilde{\gamma}\left(d(\tilde{\xi}, t_k) + \sum_{i=1}^{24} u_i \chi_{(i-1, i]}(t_k)\right)^2 - \left(p_{\text{entry}}^{\max}\right)^2 + \left(p_R^{\min}\right)^2, \end{aligned}$$

$t_k := kT/N$  and  $u = (u_1, \dots, u_{24})$ . In this way, our originally implicit probabilistic constraint in (6) turns into a standard one as in (11) upon putting  $M := 2N$  and  $\eta := \tilde{\xi}$ ,

**Table 1** Parameters and values for the numerical computations

Parameter	Value	Unit
$\alpha$	147437.68	$s^{-2}$
$\beta$	0.785398	$m^2$
$\gamma$	777.073	$m^{-1}s^{-2}$
$h$	50,000	m
$p_{\text{entry}}^{\min}$	5,800,000	$kg\ m^{-1}s^{-2}$
$p_{\text{entry}}^{\max}$	6,000,000	$kg\ m^{-1}s^{-2}$
$p_R^{\min}$	5,300,000	$kg\ m^{-1}s^{-2}$
$p_R^{\max}$	5,700,000	$kg\ m^{-1}s^{-2}$
$N$	96	–
$K$	10,000	–
$p$	0.9	–
$s$	0.012	$kg\ (MW)^{-1}s^{-1}$

where the latter random vector is Gaussian (see Sect. 2.4). Hence, based on the formulae above, the method of spherical-radial decomposition described in Sect. 2.5 can be employed in order to compute values and gradients for the probability function  $\varphi$  and, thus, numerically to solve problem (6).

### 3.2 Numerical results

For numerical illustration of the previous section, we choose the data and parameters for our problem according to Table 1.

Here, the first group of quantities relates to physical coefficients as introduced in the beginning of Sect. 2.1 (see (1) and (7)). The relevant value for  $\tilde{\gamma}$ , needed in the representation of the quasi-static case, is obtained by the formula given in (5). The second group of quantities provides the required pressure bounds in (3),  $p$  refers to the probability level chosen in problem (6) and  $s$  is the factor scaling down the demand modeled in (9) to a single pipe (see end of Sect. 2.4). All computations are done with MATLAB using the built-in SQP solver for the optimization routine `fmincon` with default settings.

The solution of the probabilistic capacity maximization problem in the case of quasi-static gas transport is displayed in Fig. 3. For nicer visualization, the optimal time-dependent free capacities are plotted as linear interpolations of the original piecewise (hourly) constant function. The probability level was chosen as  $p = 0.9$ . Not surprisingly, the profile of free capacity is somehow complementary to the typical profiles of demands of existing clients shown in Fig. 2: there is more free capacity at night time and a shallow peak is also observed around noon. In addition to the solution of the optimization problem itself, Fig. 3 shows twenty so-called *complete scenarios* the meaning of which will be made precise in Sect. 3.3. These scenarios are composed of a stochastic load scenario  $\xi$  for the demand of gas by existing clients



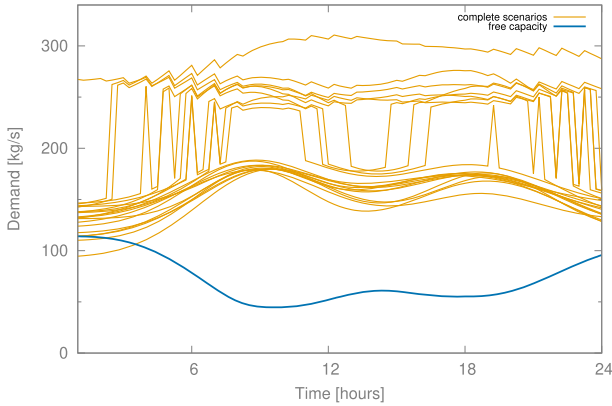


**Fig. 3** Solution of the probabilistic capacity maximization problem with probability level  $p = 0.9$  in the case of quasi-static gas transport

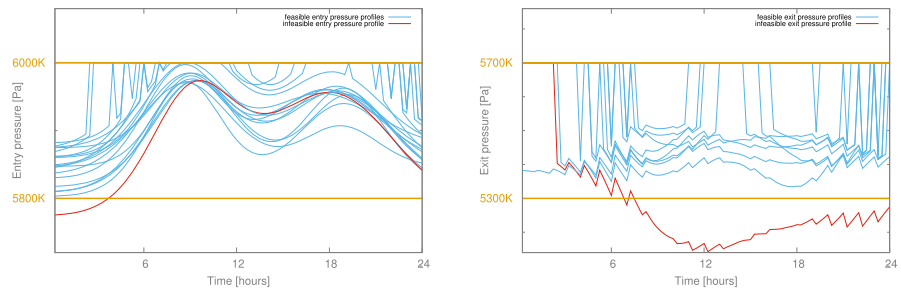


**Fig. 4** Pressure profiles at the entry (left) and exit (right) for the 20 complete load scenarios at the exit displayed in Fig. 3

plus an associated *worst case* scenario  $y^*$  for the uncertain gas load of future clients which removes the ambiguity of  $y$  with  $0 \leq y \leq U$  in (6).

We obtain that the complete scenarios partially look smooth much like the original stochastic demand scenarios from Fig. 2 and partially exhibit chaotic jumps. The latter are hardly observed in this extreme form in reality, they are just a result of reflecting the worst case behaviour of a future client. These scenarios can be used for a posterior check of the obtained solution: given the probability 0.9, for approximately 18 out of these 20 scenarios there should exist pressure profiles  $p^{\text{entry}}, p(R, \cdot)$  at the entry and exit, respectively, satisfying the pressure bound (3) as well as the quasi-static relation (5). These required pressure profiles associated with the twenty complete scenarios are displayed in Fig. 4.

We note that the construction of scenario-dependent pressure profiles is not unique. The concrete construction presented in Sect. 3.3 below is chosen in a way that the upper pressure bounds  $p_{\text{entry}}^{\text{max}}, p_R^{\text{max}}$  at the entry and exit are always satisfied, hence violations can only be observed with respect to the lower pressure bounds. According to Fig. 4, there is one profile for the entry and one profile for the exit that violates the imposed lower pressure bounds. Since they correspond to two different complete load scenarios

visualized in Fig. 3, the empirical probability for technical feasibility according to our posterior check equals 18/20 which coincides with the chosen probability level of 0.9 (in general, by repeating simulations for the posterior check, slight deviations of the empirical from the theoretical one may be expected).

### 3.3 Worst case scenarios and recovery of scenario-dependent pressure profiles

In this section we show how to recover worst case scenarios for the load  $y$  of new clients given a stochastic scenario for the load of existing clients. Moreover, the scenario-dependent profiles for the pressures  $p^{\text{entry}}, p(R, \cdot)$  at the entry and exit, given a function of free capacities and a (random) load scenario at the exit. While these constructions are not needed in the solution of the optimization problem itself thanks to Corollary 1 (which reduces the feasibility issue to an inequality system not involving these worst case or pressure profiles), it is useful for several other reasons: first, our posterior check of the computed solution relied on the mentioned pressure profiles (see Fig. 4); second, the identification of the pressure profile at the entry for a given function of free capacities and a given (say forecasted) random load of the existing clients is actually what the TSO has to provide in the daily operation of gas injection; third, the construction of the worst case load  $y$  and the pressure profile at the entry in the quasi-static case will be crucial as approximate substitutes for dealing with the worst case behaviour of future clients in the transient model of gas transport (see Sect. 3.4).

**Proposition 2** *The following equivalence holds true:*

$$q^{\text{exit}} + y \in \mathcal{T}^{\text{qstat}} \quad \forall y : [0, T] \rightarrow \mathbb{R} : 0 \leq y \leq U \iff q^{\text{exit}} + y^*(q^{\text{exit}}, U) \in \mathcal{T}^{\text{qstat}},$$

where, for  $t \in [0, T]$ ,

$$y^*(q^{\text{exit}}, U)(t) := \begin{cases} U(t), & \text{if } (p_{\text{entry}}^{\min})^2 - (p_R^{\max})^2 - \tilde{\gamma}(q^{\text{exit}}(t))^2 \leq \\ & \tilde{\gamma}(q^{\text{exit}}(t) + U(t))^2 - (p_{\text{entry}}^{\max})^2 + (p_R^{\min})^2, \\ 0, & \text{else.} \end{cases} \quad (18)$$

**Proof** Replacing  $q^{\text{exit}}$  in Proposition 1 by  $q^{\text{exit}} + y^*(q^{\text{exit}}, U)$ , we get that

$$\begin{aligned} q^{\text{exit}} + y^*(q^{\text{exit}}, U) &\in \mathcal{T}^{\text{qstat}} \\ \iff & \\ (p_{\text{entry}}^{\min})^2 - (p_R^{\max})^2 &\leq \tilde{\gamma}(q^{\text{exit}}(t) + y^*(q^{\text{exit}}, U)(t))^2, \\ \tilde{\gamma}(q^{\text{exit}}(t) + y^*(q^{\text{exit}}, U)(t))^2 &\leq (p_{\text{entry}}^{\max})^2 - (p_R^{\min})^2 \quad \forall t \in [0, T]. \end{aligned} \quad (19)$$

Hence, by Corollary 1, the equivalence claimed in our Proposition will be proven once we have shown the equivalence of the inequality systems in (19) and (17). Since

$y^*(q^{\text{exit}}, U)(t)$  is equal to 0 or to  $U(t)$ , it is easily seen that the inequalities in (17) imply those in (19). Conversely, let inequalities (19) hold true. If  $t \in [0, T]$  is such that the first case of (18) applies, then  $y^*(q^{\text{exit}}, U)(t) = U(t)$  and the second inequality in (17) follows from the second inequality in (19). In particular,

$$\tilde{\gamma} \left( q^{\text{exit}}(t) + U(t) \right)^2 - \left( p_{\text{entry}}^{\text{max}} \right)^2 + \left( p_R^{\text{min}} \right)^2 \leq 0,$$

whence the first inequality in (17) follows along with the inequality defining the first case in (18). An analogous argumentation applies if the second case in (18) holds true. □

Clearly, the discrimination between the two cases in (18) is characterized by the equality

$$\left( p_{\text{entry}}^{\text{min}} \right)^2 - \left( p_R^{\text{max}} \right)^2 - \tilde{\gamma} \left( q^{\text{exit}}(t) \right)^2 = \tilde{\gamma} \left( q^{\text{exit}}(t) + U(t) \right)^2 - \left( p_{\text{entry}}^{\text{max}} \right)^2 + \left( p_R^{\text{min}} \right)^2.$$

Resolving this equation for  $q^{\text{exit}}(t)$  and calling the solution  $\Delta$  yields

$$\Delta(t) = -\frac{U(t)}{2} + \sqrt{\frac{\left( p_{\text{entry}}^{\text{min}} \right)^2 + \left( p_{\text{entry}}^{\text{max}} \right)^2 - \left( p_R^{\text{min}} \right)^2 - \left( p_R^{\text{max}} \right)^2}{2\tilde{\gamma}} - \frac{U^2(t)}{4}}$$

(the negative sign in front of the square root being excluded because otherwise the solution would be negative). We shall call  $\Delta$  the *discriminant*, because it decides on the case distinction in (18). More precisely, we may write now

$$y^*(q^{\text{exit}}, U)(t) = \begin{cases} U(t) & \text{if } q^{\text{exit}}(t) \geq \Delta(t), \\ 0 & \text{else,} \end{cases} \quad (t \in [0, T]). \tag{20}$$

The construction of the worst case scenario according to (20) is illustrated in Fig. 5: whenever the demand scenario  $q^{\text{exit}}$  is smaller than the discriminant  $\Delta$ , then the worst case scenario  $y$  is defined to be zero, otherwise it is put equal to the capacity function  $U$ . We note that contrary to Fig. 3, where the profile of free capacities has been plotted as a linear interpolation for nicer visualization, the function is represented in Fig. 5 in its original piece-wise constant shape. This explains the jumps also in the other functions.

We will define a *complete scenario* to be the sum of a given demand scenario and the associated worst case scenario (for an illustration, see Fig. 5):

$$c(q^{\text{exit}}, U) := q^{\text{exit}} + y^*(q^{\text{exit}}, U). \tag{21}$$

The importance of this concept relies on the possibility to remove the ambiguity of the load scenario  $y$  for potential future clients in (6). Indeed, thanks to Proposition 2, we may simplify the probability in (6) as

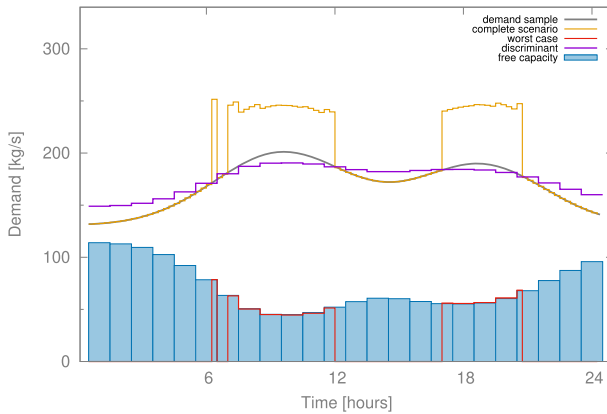


**Fig. 5** Illustration of the construction of worst case and complete scenarios based on a demand scenario and a given function of free capacities

$$\mathbb{P}(\xi + y \in \mathcal{T}^{\text{qstat}} \quad \forall y : [0, T] \rightarrow \mathbb{R} : 0 \leq y \leq U) = \mathbb{P}(c(\xi, U) \in \mathcal{T}^{\text{qstat}})$$

$$\text{for } U := \sum_{i=1}^{24} u_i \chi_{(i-1, i]}.$$

This observation justifies our posterior check for the numerical solution of our optimization problem in Sect. 3.2: one may simulate a number of  $K$  samples for the Gaussian random vector  $\xi$  which yields  $K$  samples for the demand process  $\xi = d(\xi, \cdot)$  according to (9). These, in turn, generate  $K$  complete scenarios  $c(\xi, U) := \xi + y^*(\xi, U)$  as illustrated in Fig. 3. Now, one may count the number  $\tilde{K}$  of complete scenarios belonging to the set  $\mathcal{T}^{\text{qstat}}$  by checking the constructed pressure profiles at the exit and entry as in Fig. 4. Then, the ratio  $\tilde{K}/K$  is an empirical approximation of the true probability inside (6) and should be close to the desired value  $p$  if the computed optimal function  $u$  of free capacities is feasible.

It remains to recover the scenario-dependent profiles for the pressures  $p^{\text{entry}}(\cdot)$ ,  $p(R, \cdot)$  at the entry and exit, given a function of free capacities and a (random) load scenario at the exit. The formulae for pressure recovery have actually been derived already in (16) for a general feasible load profile  $q^{\text{exit}}$  at the exit. Here, we have to apply them to a complete scenario of the form (21), where  $q^{\text{exit}}$  just represents a (random) load scenario for the existing clients which is complemented by a worst-case scenario for future clients. According to (16), we obtain that

$$p^{\text{entry}}(t) := \min \left\{ p_{\text{entry}}^{\text{max}}, \sqrt{\tilde{\gamma}(q^{\text{exit}}(t) + y^*(q^{\text{exit}}, U)(t))^2 + (p_R^{\text{max}})^2} \right\}, \quad (22)$$

$$p(R, t) := \sqrt{(p^{\text{entry}}(t))^2 - \tilde{\gamma}(q^{\text{exit}}(t) + y^*(q^{\text{exit}}, U)(t))^2}. \quad (23)$$

Using the representation of the worst-case scenario  $y^*(q^{\text{exit}}, U)$  from (18) or, equivalently, (20), one may recover now the pressure profiles at the entry and exit from

a load profile at the exit and from a given function of free capacities as was done in Fig. 4. As it is shown in the proof of Proposition 1, the two pressure profiles in (22),(23) satisfy the pressure bounds (3) whenever the underlying complete scenario is technically feasible  $(c(\xi, U) \in \mathcal{T}^{\text{qstat}})$ .

### 3.4 The transient case

As mentioned in the introduction to Sect. 3, it is hopeless in the transient case to derive a similar equivalent description of the family of inclusions

$$q^{\text{exit}} + y \in \mathcal{T}^{\text{trans}} \quad \forall y : [0, T] \rightarrow \mathbb{R} : 0 \leq y \leq U \quad \left( U = \sum_{i=1}^{24} u_i \chi_{(i-1,i)} \right) \quad (24)$$

in (6) by means of explicit inequalities as was done in Corollary 1. In particular, deriving a worst-case scenario equivalently representing (24) as in the quasi-static case (see Proposition 2) is out of reach. In order to cope with this issue, we shall assume that the quasi-static model is sufficiently close to the transient one, in order to justify the assumption that the worst-case function constructed in (18) could analogously represent the family of inclusions (24) by the single one

$$c(q^{\text{exit}}, U) := q^{\text{exit}} + y^*(q^{\text{exit}}, U) \in \mathcal{T}^{\text{trans}},$$

where we used the definition of a complete scenario from (21). Then, the probabilistic constraint in problem (6) turns into the simpler expression

$$\mathbb{P}(c(\xi, U) \in \mathcal{T}^{\text{trans}}) \geq p. \quad (25)$$

Still, the random constraint inside the probability is not explicit yet and has to be resolved as an inequality system. By definition, the relation  $c(\xi, U) \in \mathcal{T}^{\text{trans}}$  is equivalent to the existence of a pressure profile  $p^{\text{entry}}$  at the entry and a solution  $(p, q)$  of the PDE (1) satisfying the boundary and initial conditions

$$p(L, t) = p^{\text{entry}}(t); \quad q(R, t) = c(\xi, U)(t) \quad \forall t \in [0, T],$$

$$p(R, 0) = p_R^0; \quad q(L, 0) = q_L^0$$

as well as the constraints (3). Denote by  $F(p_L, q_R, p_R^0, q_L^0)$  the pressure function  $p$  associated with the unique solution  $(p, q)$  of the PDE (1) under boundary and initial conditions

$$p(L, t) = p_L(t); \quad q(R, t) = q_R(t) \quad \forall t \in [0, T], \quad p(R, 0) = p_R^0; \quad q(L, 0) = q_L^0.$$

Then, the probability in (25) can be written as

$$\mathbb{P}(c(\xi, U) \in \mathcal{T}^{\text{trans}}) = \mathbb{P}(\exists p^{\text{entry}} : [0, T] \rightarrow \mathbb{R} : p^{\text{entry}}(t) \in [p_{\text{entry}}^{\min}, p_{\text{entry}}^{\max}]; F(p^{\text{entry}}, c(\xi, U), p_R^0, q_L^0)(R, t) \in [p_R^{\min}, p_R^{\max}] \quad \forall t \in [0, T]) \tag{26}$$

The remaining problem with this representation of the probability for feasible transport is the ambiguity of the pressure profile  $p^{\text{entry}}$  at the entry. Plugging an arbitrary function here which satisfies the pressure bounds at the entry will yield a probability which is smaller than that on the left-hand side. To increase this smaller probability,  $p^{\text{entry}}$  should not just be a fixed function of time but also depend on the random load  $c(\xi, U)$ . Moreover, this functional dependence should be chosen as to maximize the probability on the right-hand side (thus making it coincide with that on the left-hand side). To find this functional dependence, which should moreover be given as an explicit formula in order to deal with the probability analytically in the framework of an optimization algorithm, appears to be hardly possible. Once more, we find a remedy in the quasi-static model where it was possible to recover pressure functions at the entry and exits from a given complete scenario such that the quasi-static transport model and the corresponding pressure bounds are satisfied whenever the underlying stochastic scenario  $\xi$  was technically feasible (see (22),(23)). The idea for the transient case is now to use the entry profile from (22) as a boundary condition in the transient model, thus removing the ambiguity in (26) by selecting a concrete function. Since  $p^{\text{entry}}$  in (22) may violate the lower pressure bound  $p_{\text{entry}}^{\min}$  (while satisfying  $p_{\text{entry}}^{\max}$  by construction) we additionally raise it up to the lower bound then, so that the scenario-dependent  $p^{\text{entry}}$  automatically satisfies the pressure bounds. Given the definition (21), (22) can be adapted to define the profile

$$p_*^{\text{entry}}(c(\xi, U)) := \max \left\{ p_{\text{entry}}^{\min}, \min \left\{ p_{\text{entry}}^{\max}, \sqrt{\tilde{\gamma} c^2(\xi, U) + (p_R^{\max})^2} \right\} \right\}. \tag{27}$$

After having fixed a profile  $p_*^{\text{entry}}$  satisfying the pressure bounds, we may approximate the probability  $\mathbb{P}(c(\xi, u) \in \mathcal{T}^{\text{trans}})$  in (26) by the probability

$$\mathbb{P}\left(F\left(p_*^{\text{entry}}(c(\xi, U)), c(\xi, U), p_R^0, q_L^0\right)(R, t) \in [p_R^{\min}, p_R^{\max}] \quad \forall t \in [0, T]\right) \tag{28}$$

which just relates to the pressure at the exit given the initial and boundary conditions. Here, the random constraints are still continuous in time. Next, we want to subordinate the random constraint inside the probability to the time discretization and the implicit Euler scheme of (7) for numerically identifying the state variables of the PDE (1). We observe first that for  $k = 1, \dots, N$  the values of the mapping  $F$  at  $t^k := kT/N$  correspond to the pressures  $p^k$  in (7). In this discretization scheme, the pressures (and flows) are associated with the discretized load  $z$  at the exit and pressure  $w$  at the entry. Our time-discrete version of (28) therefore becomes

$$\mathbb{P}\left(\tilde{F}^k\left(w(\xi, U), z(\xi, U), p_R^0, q_L^0\right) \in [p_R^{\min}, p_R^{\max}]; \quad k = 1, \dots, N\right), \tag{29}$$

where  $\tilde{F}^k(w(\xi, U), z(\xi, U), p_R^0, q_L^0)$  refers to the value  $p^k$  in the scheme (7) obtained with initial conditions  $p^0 := p_R^0$  and  $q^0 := q_L^0$  and boundary values  $w, z$  defined by

$$z^k(\xi, U) := c(\xi, U)(t_k), \quad w^k(\xi, U) := p_*^{\text{entry}}(c(\xi, U))(t_k), \quad k = 1, \dots, N.$$

In order to remove the functional character of the right-hand side expressions, we recall from (18) that

$$y^*(q^{\text{exit}}, U)(t) = \psi_1(q^{\text{exit}}(t), U(t)) \quad \forall t \in [0, T],$$

where

$$\psi_1(\alpha, \beta) := \begin{cases} \beta, & \text{if } (p_{\text{entry}}^{\min})^2 - (p_R^{\max})^2 - \tilde{\gamma}\alpha^2 \leq \tilde{\gamma}(\alpha + \beta)^2 - (p_{\text{entry}}^{\max})^2 + (p_R^{\min})^2 \\ 0, & \text{elsewhere} \end{cases}$$

Accordingly, (21) yields that

$$c(\xi, U)(t) = \xi(t) + \psi_1(\xi(t), U(t)).$$

Similarly, we derive from (27) that

$$p_*^{\text{entry}}(c(\xi, U))(t) = \psi_2(c(\xi, U)(t));$$

$$\psi_2(\tau) := \max \left\{ p_{\text{entry}}^{\min}, \min \left\{ p_{\text{entry}}^{\max}, \sqrt{\tilde{\gamma}\tau^2 + (p_R^{\max})^2} \right\} \right\}.$$

Summarizing, for  $k = 1, \dots, N$  we have that

$$z^k(\xi, U) = \xi(t_k) + \psi_1(\xi(t_k), U(t_k)); \quad w^k(\xi, U) = \psi_2(\xi(t_k) + \psi_1(\xi(t_k), U(t_k))).$$

In the last step, we take into account the concrete representation  $\xi = d(\tilde{\xi}, \cdot)$  of our random process according to (9), so that randomness enters via the finite-dimensional Gaussian random vector  $\tilde{\xi}$ . This leads us to define for  $k = 1, \dots, N$ :

$$\hat{z}^k(\tilde{\xi}, U) := z^k(\xi, U) = d(\tilde{\xi}, t_k) + \psi_1(d(\tilde{\xi}, t_k), U(t_k)) \tag{30}$$

$$\hat{w}^k(\tilde{\xi}, U) := w^k(\xi, U) = \psi_2(d(\tilde{\xi}, t_k) + \psi_1(d(\tilde{\xi}, t_k), U(t_k))) \tag{31}$$

In this way, the probability in (29) can be written in the form of (11) amenable to spherical-radial decomposition upon setting  $M := 2N$ ,  $u := (u_1, \dots, u_{24})$ ,  $\eta := \tilde{\xi}$ , and for  $k = 1, \dots, N$ :

$$g_k(u, \tilde{\xi}) := p_R^{\min} - \tilde{F}^k \left( \hat{w} \left( \tilde{\xi}, \sum_{i=1}^{24} u_i \chi_{(i-1, i]} \right), \hat{z} \left( \tilde{\xi}, \sum_{i=1}^{24} u_i \chi_{(i-1, i]} \right), p_R^0, q_L^0 \right)$$

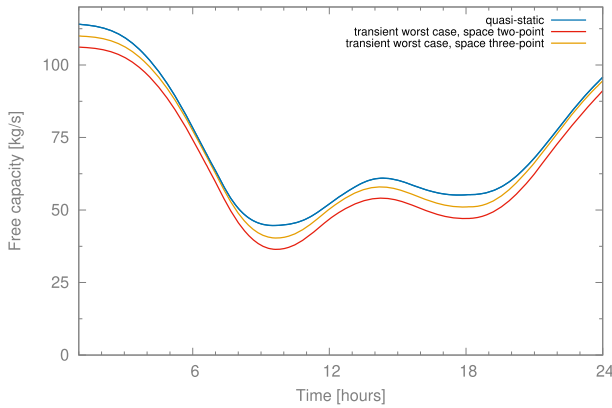


**Fig. 6** Comparison of the maximum capacities in a single pipe computed for the quasi-static and transient model, respectively. The transient computations are related to a two-point and an advanced three-point space discretization, respectively

$$g_{N+k}(u, \tilde{\xi}) := \tilde{F}^k \left( \hat{w} \left( \tilde{\xi}, \sum_{i=1}^{24} u_i \chi_{(i-1,i]} \right), \hat{z} \left( \tilde{\xi}, \sum_{i=1}^{24} u_i \chi_{(i-1,i]} \right), p_R^0, q_L^0 \right) - p_R^{\max}.$$

Observe that the functions  $g_k$  are fully explicit via (30), (31) upon taking into account that in these formulae

$$U(t_k) = \sum_{i=1}^{24} u_i \chi_{(i-1,i]}(t_k) \quad k = 1, \dots, N.$$

We may therefore apply the method of spherical-radial decomposition presented in Sect. 2.5 in order to calculate the probabilistic constraint inside the optimization problem (6). As pointed out in Sect. 2.5, an efficient numerical treatment of the optimization problem will also require the gradient of this probability as a function of the decision vector  $u$ . This can be done with the aid of formula (14). As described below this formula, it will be necessary to calculate the partial gradients with respect to  $u$  and  $\eta = \tilde{\xi}$  of the constraint functions  $g_k$ . This can be realized using the explicit formulae for these functions provided above. More precisely, the gradients for  $\hat{z}$  and  $\hat{w}$  follow from (30) and (31), respectively, whereas the gradient of  $\tilde{F}^k$  (playing the role of  $p^k$  in the implicit Euler scheme (7)) can be computed via the updating formula (8).

Figure 6 illustrates the solution of the probabilistic capacity maximization problem in the case of transient gas flow. It can be seen that a small deviation of the solution based on the two-point discretization scheme (7) from the solution of the quasi-static model of gas transport (the same as in Fig. 3) appears. However, when passing to a finer three-point discretization in space, this small gap is further reduced such that the deviation is widely negligible. This confirms the fact that the solutions in the transient and quasi-static models almost coincide.



### 4 Probabilistic capacity maximization in a network with tree structure

In this section we want to generalize the ideas related with a single pipe and presented in the previous section to a general network. As before, we shall first deal with the quasi-static model of gas transport. We shall keep the assumption of dealing with a single entry only at which gas is injected, whereas there may be several exits now at which gas is withdrawn for consumption. We shall further assume that the network is a tree. This would not be necessary for a generalization of Proposition (1) which addresses the reformulation of technical feasibility of exit-loads  $\xi$  by means of an explicit inequality system. Indeed, such inequality system would have to be complemented by certain equations in additional variables corresponding to fundamental cycles in the network (see, Gotzes et al. (2016) Theorem 1). A corresponding result incorporating unknown loads  $y$  of potentially new customers along the lines of Corollary 1 appears to be hardly possible in the presence of cycles. Therefore, we restrict our presentation to networks with tree structure from the very beginning, in which case the generalization of Proposition 1 too can be given in the form of an inequality system only.

#### 4.1 Transport model for a tree

We shall assume that our gas network is a directed and contains  $G + 1$  nodes, where the root node '0' is identified with the (single) entry and nodes '1' to 'G' correspond to the exits. We denote the set of arcs in the tree by  $\mathcal{E}$  and the arc-dependent coefficients  $\tilde{\gamma}$  from (4) by  $\tilde{\gamma}_{k,l}$  (for  $(k, l) \in \mathcal{E}$ ). Moreover, we assume that all arcs in  $\mathcal{E}$  are directed away from the root. To describe the network topology we introduce the (reduced) node-arc incidence matrices  $A_L, A_R \in \mathbb{R}^{G \times |\mathcal{E}|}$  defined by  $(A_L)_{ke} := -1$  if node  $k$  is left node of arc  $e$  and  $(A_L)_{ke} := 0$  otherwise, and,  $(A_R)_{ke} := +1$  if node  $k$  is right node of arc  $e$  and  $(A_R)_{ke} := 0$  otherwise ( $k = 1, \dots, G; e \in \mathcal{E}$ ). When dealing with the transient gas flow in a tree network we are going to apply a priori the *two-point space discretization* of the isothermal Euler equations (1) for each pipe of the given network.

Before starting the analysis, the meaning of 'technical feasibility' from Definitions 1 and 2 have to be generalized from a single pipe to the network.

**Definition 3** A vector of load profiles  $q^{\text{exit}} = (q_1^{\text{exit}}, \dots, q_G^{\text{exit}})$  for gas withdrawal at the exits will be said to be technically feasible w.r.t. **transient** gas flow if there exist vectors of pressure and flow profiles  $p_L, p_R$  and  $q_L, q_R$  along the directed arcs of  $\mathcal{E}$ , where each component is either the left/right pressure or the left/right flow of a certain pipe, respectively; solving component-wise (for each arc  $e \in \mathcal{E}$ )

$$\begin{aligned} \partial_t p_R + \frac{\alpha}{h} (q_R - q_L) &= 0 \\ \partial_t q_L + \frac{\beta}{h} (p_R - p_L) + \gamma \frac{q_L |q_L|}{p_R} &= 0 \end{aligned} \quad \forall t \times [0, T], \tag{32}$$

satisfying the flow balance equation

$$A_L q_L + A_R p_R = q^{\text{exit}} \quad \forall t \in [0, T].$$

Moreover, there exist a vector of pressure profiles  $p = (p_0, \dots, p_G)$  at the entry and all exit nodes, respectively, satisfying the coupling constraints

$$p_L^{(k,l)} = p_R^{(m,k)} = p_k \quad \forall t \in [0, T]; \quad k = 0, \dots, G; \quad \forall (m, k), (k, l) \in \mathcal{E},$$

and the pressure bounds

$$p_k(t) \in [p_k^{\min}, p_k^{\max}] \quad \forall t \in [0, T]; \quad k = 0, \dots, G.$$

**Definition 4** A vector of load profiles  $q^{\text{exit}} = (q_1^{\text{exit}}, \dots, q_G^{\text{exit}})$  for gas withdrawal at the exits will be said to be technically feasible w.r.t. **quasi-static** gas flow if there exist a vector of pressure profiles  $p = (p_0, \dots, p_G)$  at the entry and all the exits, respectively, and a vector  $f = (f_{k,l})$  of flow profiles along the directed arcs  $(k, l) \in \mathcal{E}$  satisfying the pressure drop equations

$$p_k^2(t) - p_l^2(t) = \tilde{\gamma}_{k,l} f_{k,l}(t) |f_{k,l}(t)| \quad (t \in [0, T]; \quad (k, l) \in \mathcal{E}),$$

the Kirchhoff law

$$\sum_{\{l:(l,k) \in \mathcal{E}\}} f_{l,k} - \sum_{\{l:(k,l) \in \mathcal{E}\}} f_{k,l} = q_k^{\text{exit}} \quad \forall t \in [0, T]; \quad k = 0, \dots, G,$$

as well as the pressure bounds

$$p_k(t) \in [p_k^{\min}, p_k^{\max}] \quad \forall t \in [0, T]; \quad k = 0, \dots, G.$$

The definitions of the sets  $\mathcal{T}^{\text{trans}}, \mathcal{T}^{\text{qstat}}$  will remain the same as in the case of a single pipe except that they now refer to Definitions 3 and 4 in the context of a network.

### 4.2 The quasi-static case

In this section we are going to generalize the results of Sect. 3.1 from a single pipe to a tree-like network as introduced above. Our probabilistic capacity maximization problem with quasi-static gas transport along a tree with an entry as root node '0' and exit nodes '1' to 'G' now reads as

$$\begin{aligned} & \max_{(u_k^i)_{i,k \in \mathbb{R}_+^{24 \times G}}} \sum_{k=1}^G \sum_{i=1}^{24} u_k^i \quad \text{subject to} \\ & \mathbb{P}\left(\xi + y \in \mathcal{T}^{\text{qstat}} \quad \forall y : [0, T] \rightarrow \mathbb{R}^G : 0 \leq y_k \leq \sum_{i=1}^{24} u_k^i \chi_{(i-1,i)}; \quad k = 1, \dots, G\right) \geq p. \end{aligned} \tag{33}$$

Here, the array  $(u_k^i)_{i=1,\dots,24;k=1,\dots,G}$  represents the hourly discretized free capacities at the exit nodes  $k = 1, \dots, G$  corresponding at node  $k$  to the function of time

$$U_k(t) = \sum_{i=1}^{24} u_k^i \chi_{(i-1,i]}(t). \tag{34}$$

To start with, Proposition 1 generalizes as

**Proposition 3** For a given vector  $q^{\text{exit}} = (q_1^{\text{exit}}, \dots, q_G^{\text{exit}}) \geq 0$  of exit load profiles, the following equivalence holds true:

$$q^{\text{exit}} \in \mathcal{T}^{\text{qstat}} \iff h_k(q^{\text{exit}}(t)) + (p_k^{\text{max}})^2 - h_l(q^{\text{exit}}(t)) - (p_l^{\text{min}})^2 \geq 0 \quad \forall k, l = 0, \dots, G \quad \forall t \in [0, T],$$

where

$$h_k(z) := \sum_{e \in \Pi(k)} \tilde{\gamma}_e \left( \sum_{m \geq H(e)} z_m \right)^2$$

Here,  $\Pi(k)$  denotes the unique directed path from the root to node  $k$ , where for the root itself we put  $\Pi(0) := \emptyset$ . In particular,  $h_0 \equiv 0$ . The relation  $k \geq l$  for  $k, l \in \{0, \dots, G\}$  means that  $\Pi(k)$  passes through  $l$ .  $H(e)$  refers to the head of the (directed) arc  $e \in \mathcal{E}$ .

**Proof** This result has been shown for a stationary flow model (no time involved) in (Gotzes et al. (2016) Corollary 1). In the quasi-static model considered here, stationarity is assumed at each time  $t \in [0, T]$ , hence the result is just applied point-wise in time. □

The proposition shows how to equivalently reformulate in the quasi-static network model the technical feasibility of a vector of general load profiles as an explicit system of inequalities. The incorporation of unknown loads  $y$  in the limits of free capacities cannot be derived as easily as in Corollary 1 for a single pipe. Nonetheless, we have the following

**Proposition 4** For a given vector  $q^{\text{exit}} = (q_1^{\text{exit}}, \dots, q_G^{\text{exit}}) \geq 0$  of exit load profiles and a given vector  $U = (U_1, \dots, U_G) \geq 0$  of time-dependent free capacities at the exits the following equivalence holds true:

$$q^{\text{exit}} + y \in \mathcal{T}^{\text{qstat}} \quad \forall y : [0, T] \rightarrow \mathbb{R}^G : 0 \leq y \leq U$$

$$\iff \alpha_{k,l}(q^{\text{exit}}, U, t) \geq 0 \quad \forall k, l = 0, \dots, G \quad \forall t \in [0, T],$$

where, for  $k, l = 0, \dots, G$  and  $t \in [0, T]$ ,

$$\alpha_{k,l}(q^{\text{exit}}, U, t) := \sum_{e \in \Pi(k) \setminus \Pi(l)} \tilde{\gamma}_e \left( \sum_{s \geq H(e)} q_s^{\text{exit}}(t) \right)^2 + (p_k^{\text{max}})^2$$

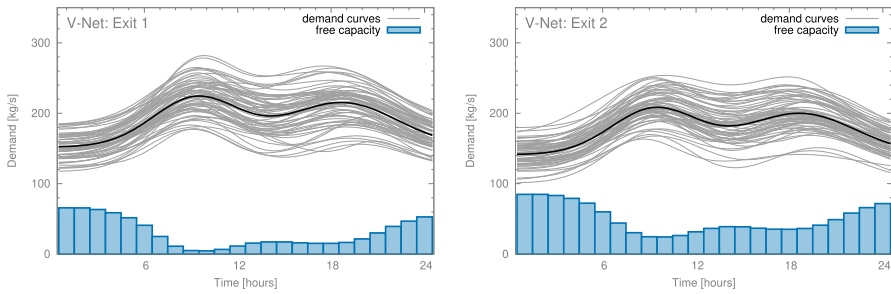


**Fig. 7** Solution of the capacity problem (33) computed by the quasi-static model obtained for exit 1 (left) and exit 2 (right) for a V-net containing a single entry and two exit nodes

$$- \sum_{e \in \Pi(l) \setminus \Pi(k)} \tilde{\gamma}_e \left( \sum_{s \geq H(e)} q_s^{\text{exit}}(t) + U_s(t) \right)^2 - (p_l^{\min})^2.$$

**Proof** Again, the corresponding result has been proven in (Heitsch (2020) Sect. 3.2) for a stationary flow model and it follows in the quasi-static case by applying it pointwise in time.  $\square$

Equipped with the result of the previous proposition and passing to a time discretization of the form  $t_j := j * T / N$  for  $j = 1, \dots, N$  as in the case of a single pipe, we may rewrite the probabilistic constraint in our optimization problem (33) again in the standard form of (11). To this aim, we exploit a statistical model

$$\tilde{\xi}_k(t) = d(\tilde{\xi}_k, t) \quad \forall t \in [0, T] \tag{35}$$

for the random load at each exit node  $k = 1, \dots, G$  of the tree much like we did in Sect. 2.4 for a single exit. Here,  $\tilde{\xi} = (\tilde{\xi}_k)_{k=1}^G$  is a Gaussian random vector. Now, we put for  $k, l = 0, \dots, G$  and  $j = 1, \dots, N$

$$\begin{aligned} g_{k,l,j}(u, \tilde{\xi}) := & \sum_{e \in \Pi(l) \setminus \Pi(k)} \tilde{\gamma}_e \left( \sum_{s \geq H(e)} d(\tilde{\xi}_s, t_j) + \sum_{i=1}^{24} u_s^i \chi_{(i-1,i]}(t_j) \right)^2 + (p_l^{\min})^2 \\ & - \sum_{e \in \Pi(k) \setminus \Pi(l)} \tilde{\gamma}_e \left( \sum_{s \geq H(e)} d(\tilde{\xi}_s, t_j) \right)^2 - (p_k^{\max})^2, \end{aligned}$$

and, observe that indeed the probabilistic constraint in (33) is in the standard form of (11) with  $\eta := \tilde{\xi}$  and  $M := (G + 1)^2 N$ . As in the case of a single pipe, the method of spherical-radial decomposition described in Sect. 2.5 can be employed in order to compute values and gradients for the probability function  $\varphi$  and, thus, numerically to solve problem (33).

Figure 7 shows the solution of the capacity maximization according to problem (33) for a small tree example (V-net) with two exit nodes  $G = \{1, 2\}$  involving two arcs that origin from the single entry node, i.e. the set of edges is given by  $\mathcal{E} = \{(0, 1), (0, 2)\}$ . For the exit demands we used the same fitting as given in Sect. 2.4 but with slightly

varying scaling between exit node one and two. Moreover, a randomly obtain small correlation between both exits is considered in the numerical example. The results are comparable two that of the single pipe before. Due to the different scaling of the demand curves, the capacity at exit one turns out to be a bit smaller than the capacity at exit two. This could be expected because the average demand at exit one is assumed to be higher along the overall time horizon in this example.

### 4.3 Worst case scenarios and recovery of scenario-dependent pressure profiles

In this section we generalize the results of Sect. 3.3 to a network with tree structure.

**Proposition 5** *For a given vector  $q^{\text{exit}} = (q_1^{\text{exit}}, \dots, q_G^{\text{exit}}) \geq 0$  of exit load profiles and a given vector  $U = (U_1, \dots, U_G) \geq 0$  of time-dependent free capacities at the exits the following equivalence holds true:*

$$q^{\text{exit}} + y \in \mathcal{T}^{\text{qstat}} \quad \forall y : [0, T] \rightarrow \mathbb{R}^G : 0 \leq y \leq U \iff q^{\text{exit}} + y^*(q^{\text{exit}}, U) \in \mathcal{T}^{\text{qstat}},$$

where, for  $s = 1, \dots, G$  and  $t \in [0, T]$ ,

$$[y^*(q^{\text{exit}}, U)]_s(t) := \begin{cases} U_s(t), & \text{if } s \geq H(e) \text{ for some } e \in \Pi(l^*(q^{\text{exit}}, U, t)) \setminus \Pi(k^*(q^{\text{exit}}, U, t)) \\ 0, & \text{otherwise} \end{cases}$$

and  $l^*(q^{\text{exit}}, U, t), k^*(q^{\text{exit}}, U, t) \in \{0, \dots, G\}$  are chosen such that

$$\alpha_{k^*(q^{\text{exit}}, U, t), l^*(q^{\text{exit}}, U, t)}(q^{\text{exit}}, U, t) \leq \alpha_{k, l}(q^{\text{exit}}, U, t) \quad \forall k, l \in \{0, \dots, G\}$$

holds true for the functions  $\alpha_{k, l}$  defined in Proposition 4.

**Proof** ( $\implies$ ) This direction is obvious, by construction  $y^*(q^{\text{exit}}, U)$  satisfies  $0 \leq y^*(q^{\text{exit}}, U) \leq U$ .

( $\impliedby$ ) By assumption and by Proposition 3 (applied to  $q^{\text{exit}} + y^*(q^{\text{exit}}, U)$  rather than  $q^{\text{exit}}$ ) we have that, for all  $k, l = 0, \dots, G$  and  $t \in [0, T]$ ,

$$h_k(q^{\text{exit}}(t) + y^*(q^{\text{exit}}, U)(t)) + (p_k^{\text{max}})^2 - h_l(q^{\text{exit}}(t) + y^*(q^{\text{exit}}, U)(t)) - (p_l^{\text{min}})^2 \geq 0. \tag{36}$$

The definition of  $h_k$  implies that, for  $k = 0, \dots, G$  and  $t \in [0, T]$ ,

$$h_k(q^{\text{exit}}(t) + y^*(q^{\text{exit}}, U)(t)) = \sum_{e \in \Pi(k)} \tilde{\gamma}_e \left( \sum_{s \geq H(e)} q_s^{\text{exit}}(t) + [y^*(q^{\text{exit}}, U)]_s(t) \right)^2. \tag{37}$$

We fix an arbitrary  $t \in [0, T]$  and put shortly  $k^* := k^*(q^{\text{exit}}, U, t)$  and  $l^* := l^*(q^{\text{exit}}, U, t)$  for the indices introduced in the statement of this Proposition. Then, (36) and (37) along with the definition of the paths  $\Pi(k)$  yield that

$$\begin{aligned}
 0 &\leq (p_{k^*}^{\max})^2 + h_{k^*}(q^{\text{exit}}(t) + y^*(q^{\text{exit}}, U)(t)) \\
 &\quad - h_{l^*}(q^{\text{exit}}(t) + y^*(q^{\text{exit}}, U)(t)) - (p_{l^*}^{\min})^2 \\
 &= (p_{k^*}^{\max})^2 + \sum_{e \in \Pi(k^*) \setminus \Pi(l^*)} \tilde{\gamma}_e \left( \sum_{s \geq H(e)} q_s^{\text{exit}}(t) + [y^*(q^{\text{exit}}, U)]_s(t) \right)^2 \\
 &\quad - \sum_{e \in \Pi(l^*) \setminus \Pi(k^*)} \tilde{\gamma}_e \left( \sum_{s \geq H(e)} q_s^{\text{exit}}(t) + [y^*(q^{\text{exit}}, U)]_s(t) \right)^2 - (p_{l^*}^{\min})^2.
 \end{aligned}$$

We claim the following two relations:

$$\begin{aligned}
 [y^*(q^{\text{exit}}, U)]_s(t) &= 0 && \forall s \geq H(e) \quad \forall e \in \Pi(k^*) \setminus \Pi(l^*), \\
 [y^*(q^{\text{exit}}, U)]_s(t) &= u_s(t) && \forall s \geq H(e) \quad \forall e \in \Pi(l^*) \setminus \Pi(k^*).
 \end{aligned}$$

The second relation follows immediately from the definition of  $y^*(q^{\text{exit}}, U)$ . As for the first one, let  $e^* \in \Pi(k^*) \setminus \Pi(l^*)$  and  $s \geq H(e^*)$  be arbitrarily given. Then, the path  $\Pi(s)$  leading to node  $s$  contains the edge  $e^*$ . Assume that also there exists some edge  $e' \in \Pi(l^*) \setminus \Pi(k^*)$  with  $s \geq H(e')$ . Then, the path  $\Pi(s)$  leading to node  $s$  also contains the edge  $e'$ . The edges  $e^*$  and  $e'$  do not coincide, they are both on the unique path  $\Pi(s)$ , yet neither follows nor precedes the other, which is not possible. Hence, there cannot exist any  $e \in \Pi(l^*) \setminus \Pi(k^*)$  with  $s \geq H(e)$ . From the definition of  $y^*(q^{\text{exit}}, u)$  we derive the first relation.

Now, with the proven two relations and exploiting the definitions of the indices  $k^*, l^*$  in the statement of this proposition, we may continue the estimation above by

$$\begin{aligned}
 0 &\leq (p_{k^*}^{\max})^2 + \sum_{e \in \Pi(k^*) \setminus \Pi(l^*)} \tilde{\gamma}_e \left( \sum_{s \geq H(e)} q_s^{\text{exit}}(t) \right)^2 \\
 &\quad - \sum_{e \in \Pi(l^*) \setminus \Pi(k^*)} \tilde{\gamma}_e \left( \sum_{s \geq H(e)} q_s^{\text{exit}}(t) + U_s(t) \right)^2 - (p_{l^*}^{\min})^2 \\
 &= \alpha_{k^*, l^*}(q^{\text{exit}}, U, t) \leq \alpha_{k, l}(q^{\text{exit}}, U, t) \quad \forall k, l \in \{0, \dots, G\}.
 \end{aligned}$$

Since  $t \in [0, T]$  has been arbitrarily fixed, the assertion now follows from Proposition 4. □

Next, we follow the concept relying on the possibility to remove the ambiguity of the load scenario  $y$  for potential future clients in (33), similarly as in the single pipe implementation before. Therefore, we define the *complete scenario* again to be the sum of a given demand scenario and the associated worst case scenario:

$$c(q^{\text{exit}}, u) := q^{\text{exit}} + y^*(q^{\text{exit}}, U). \tag{38}$$

Thanks to Proposition 5, we may simplify the probability in (33) as

$$\begin{aligned} &\mathbb{P}\left(\xi + y \in \mathcal{T}^{\text{qstat}} \forall y : [0, T] \rightarrow \mathbb{R}^G : 0 \leq y_k \leq U_k, k = 1, \dots, G\right) \\ &= \mathbb{P}\left(c(\xi, U) \in \mathcal{T}^{\text{qstat}}\right) \quad \text{for } U_k := \sum_{i=1}^{24} u_k^i \chi_{(i-1, i]}, k = 1, \dots, G. \end{aligned}$$

It remains to recover the scenario-dependent profiles for the pressures  $p_0(\cdot), p_k(R, \cdot)$  at the entry and exits ( $k = 1, \dots, G$ ), given a function of free capacities and a (random) load scenario at the exit.

**Proposition 6** *Let  $q^{\text{exit}} = (q_1^{\text{exit}}, \dots, q_G^{\text{exit}}) \geq 0$  be a technically feasible vector of exit load profiles  $q^{\text{exit}} \in \mathcal{T}^{\text{qstat}}$ . Then, the vectors of pressure and flow profiles defined as*

$$\begin{aligned} p_0(t) &:= \min_{k \in \{0, \dots, G\}} \left( h_k(q^{\text{exit}}(t)) + (p_k^{\text{max}})^2 \right)^{\frac{1}{2}} \\ p_k(t) &:= \left( (p_0(t))^2 - h_k(q^{\text{exit}}(t)) \right)^{\frac{1}{2}} \quad (k = 1, \dots, G) \\ f_{k,l}(t) &:= \sum_{m \geq l} q_m^{\text{exit}}(t) \quad ((k, l) \in \mathcal{E}) \end{aligned}$$

are satisfying the pressure drop equations, the Kirchhoff law and the pressure bounds given in Definition 4;  $h_k(\cdot)$  is as given in Proposition 3.

**Proof** The result follows from the more general proof of (Gotzes et al. (2016) Theorem 1) applied for a tree network, and, applied point-wise in time for each  $t \in [0, T]$ .  $\square$

The formulae for pressure recovery for a general feasible load profile  $q_{\text{exit}}$  at the exits, given by the proposition, have to apply to a complete scenario of the form (38) again. Accordingly, we obtain that

$$p_0(t) := \sqrt{\min_{k \in \{0, \dots, G\}} h_k(q^{\text{exit}}(t) + y^*(q^{\text{exit}}, U)(t)) + (p_k^{\text{max}})^2}, \tag{39}$$

$$p_k(t) := \sqrt{(p_0(t))^2 - h_k(q^{\text{exit}}(t) + y^*(q^{\text{exit}}, U)(t))} \quad (k = 1, \dots, G). \tag{40}$$

The formulae (39) and (40) for the pressures at the entry and exits generalize formulae (22) and (23) obtained for a single pipe before. By applying the representation of the worst-case scenario  $y^*(q^{\text{exit}}, U)$  from Proposition 5, a recovering of the pressure profiles at the entry and exits from a given load profile at the exits and from a given function of free capacities is possible in a tree network situation as well.

#### 4.4 The transient case

The probabilistic capacity maximization problem with transient gas transport along a tree is formulated as in (33), where  $\mathcal{T}^{\text{qstat}}$  is replaced by  $\mathcal{T}^{\text{trans}}$ . The probabilistic constraint in the transient case reads

$$\mathbb{P}\left(q^{\text{exit}} + y \in \mathcal{T}^{\text{trans}} \forall y: [0, T] \rightarrow \mathbb{R}^G : 0 \leq y \leq U\right) \geq p, \tag{41}$$

where  $U = (U_1, \dots, U_G)$  and the  $U_k$  are defined in (34). As already stated for the single pipe, to derive a description of the conditions inside the probabilistic constraint in terms of a family of inclusions, as in the quasi-static case, is hopeless in the transient case even more when considering a tree network. Instead of that, we assume that the quasi-static model is sufficiently close to the transient model for more complex network structures than a single pipe as well. In particular, under this assumption the worst-case function introduced in Proposition 5 may represent the system of inclusions in (41) by the single condition

$$c(q^{\text{exit}}, U) := q^{\text{exit}} + y^*(q^{\text{exit}}, U) \in \mathcal{T}^{\text{trans}},$$

where we apply the tree version of the complete scenario definition from (38). Therefore, for a tree network the probabilistic capacity problem in the transient case is formulated as follows:

$$\max_{(u_k^i)_{i,k \in \mathbb{R}^{24 \times G}_+}} \sum_{k=1}^G \sum_{i=1}^{24} u_k^i \quad \text{subject to} \quad \mathbb{P}(c(\xi, U) \in \mathcal{T}^{\text{trans}}) \geq p. \tag{42}$$

We want to resolve the still non-explicit random constraint inside the probability as an inequality system similar as done for the single pipe in Sect. 3.4 before. By definition, the relation  $c(\xi, U) \in \mathcal{T}^{\text{trans}}$  is now equivalent to the existence of vectors of profiles  $p_L, p_R$  and  $q_L, q_R$  solving component-wise the PDE (32) and the existence of a vector of profiles  $p$  satisfying the boundary conditions

$$\begin{aligned} A_L q_L + A_R p_R &= c(\xi, U) \quad \forall t \in [0, T] \\ p_L^{(k,l)} &= p_R^{(m,k)} = p_k \quad \forall k = 0, \dots, G; \forall (m, k), (k, l) \in \mathcal{E}. \end{aligned}$$

According to the degree of freedom, under these boundary conditions the PDE (32) has a unique solution if we consider the additional boundary and initial conditions

$$p_0(t) = p_{\text{entry}}(t) \quad \forall t \in [0, T]; \quad p_k(0) = p_k^0, \quad k = 1, \dots, G; \quad q_L(0) = q_L^0.$$

When denoting by  $F(p_0, c(\xi, U), p^0, q_L^0)$  the pressure function  $(p_1, \dots, p_G)$  associated with the unique solution, then the probability in (42) can be written as

$$\begin{aligned} \mathbb{P}(c(\xi, U) \in \mathcal{T}^{\text{trans}}) &= \mathbb{P}\left(\exists p_0 : [0, T] \rightarrow \mathbb{R} : p_0(t) \in [p_0^{\min}, p_0^{\max}]; \right. \\ &\left. [F(p_0, c(\xi, U), p^0, q_L^0)]_k \in [p_k^{\min}, p_k^{\max}] \forall t \in [0, T]; k = 1, \dots, G\right). \end{aligned} \tag{43}$$

Just like in the single pipe problem, also in the tree formulation the probability is affected by the choice of the pressure profile  $p_0(\cdot)$  at the entry. We are aiming to maximize the probability level on the right-hand side. Instead of determining the



profile  $p_0(\cdot)$  inside the optimization framework (which is hardly possible) the idea once more is to make use of the opportunity to recover pressure functions at the entry and exits in the quasi-static model. This suggests to use the entry profile from (39) for the complete scenario as boundary condition in the transient model. To make sure to satisfy the pressure bounds the pressure profile at the entry is eventually cut at the lower bound (the upper bound is satisfied automatically). According to (39) we define the profile

$$p_0^*(c(\xi, u)) := \max \left\{ p_0^{\min}, \sqrt{\min_{k \in \{0, \dots, G\}} h_k(q^{\text{exit}}(t) + y^*(q^{\text{exit}}, u)(t)) + (p_k^{\max})^2} \right\}. \tag{44}$$

By the fixed entry pressure profile  $p_0^*$  the probability  $\mathbb{P}(c(\xi, u) \in \mathcal{T}^{\text{trans}})$  in (43) is approximated by the probability

$$\mathbb{P} \left( [F(p_0^*(c(\xi, U)), c(\xi, U), p^0, q_L^0)(t)]_l \in [p_l^{\min}, p_l^{\max}] \quad \forall t \in [0, T]; l = 1, \dots, G \right) \tag{45}$$

that relates to the pressure bound conditions at the exits for the given initial and boundary conditions. In order to transform the random constraints in (45) from continuous in time to time discrete we may apply the implicit Euler scheme (7) for solving the system of PDEs (32) (for each pipe). Based on some time discretization  $t^k := kT/N$  with  $k = 1, \dots, N$  the solution mapping  $F$  is replaced by the mappings  $\tilde{F}_l^k(p_0^*(c(\xi, U)), c(\xi, U), p^0, q_L^0)$  which denote the  $l$ -th component of the numerical solution vector  $(p_1^k, \dots, p_G^k)$  of exit pressures at time steps  $k = 1, \dots, N$ , given the corresponding initial and boundary values. The analog formula to (29) reads now:

$$\mathbb{P} \left( \tilde{F}_l^k(p_0^*(c(\xi, U)), c(\xi, U), p^0, q_L^0) \in [p_l^{\min}, p_l^{\max}]; k = 1, \dots, N; l = 1, \dots, G \right). \tag{46}$$

Now we can proceed as shown in Sect. 3.4 in details for the example of a single pipe, in order to reformulate the condition within the probability (46) in terms of a finite system of well-defined explicit inequalities. The inequalities are obtained formally as system with a number of  $2NG$  inequalities

$$\begin{aligned} g_l^k(u, \tilde{\xi}) &:= p_l^{\min} - \tilde{F}_l^k(p_0^*(c(\xi, U)), c(\xi, U), p^0, q_L^0) \leq 0 \\ g_l^{N+k}(u, \tilde{\xi}) &:= \tilde{F}_l^k(p_0^*(c(\xi, U)), c(\xi, U), p^0, q_L^0) - p_l^{\max} \leq 0 \end{aligned}$$

for  $k = 1, \dots, N$  and  $l = 1, \dots, G$ . Plugging in the formula (35) for the demand  $\xi$ , formula (38) for the complete scenario  $c(\xi, u)$  (applying the definition of the worst case  $y^*$  in Proposition 5), and, formula (44) for the worst case entry pressure  $p_0^*$ ; the above inequality system becomes fully explicit. By doing so, we are able to apply the method of spheric-radial decomposition presented in Sect. 2.5 in order to compute

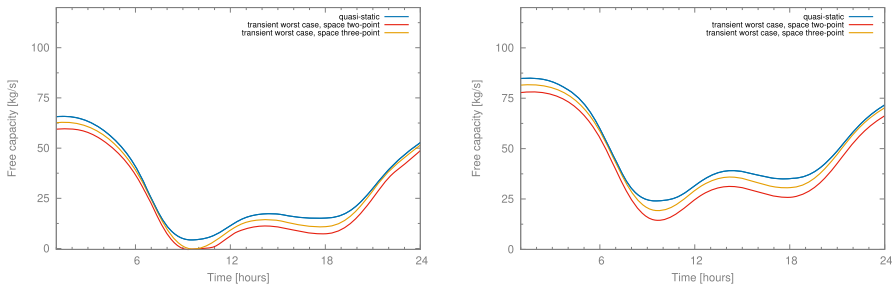


**Fig. 8** Comparison of the numerical solutions of the capacity maximization for the quasi-static and transient model using the V-net tree example. Displayed are the results for exit 1 (left) and exit 2 (right). The yellow curves refer to an advanced three-point space discretization by subdividing the two pipes of the V-net into two segments each

the probabilistic constraint inside the optimization problem (42) related to the general transient case.

We want to conclude this section by the comparison of the numerical solutions of the problem of maximizing the free capacity which are obtained by the quasi-static and by the transient model, respectively. In the single pipe example we have already made the observation that the difference between the two solutions is reasonable small (see Fig. 6), in particular, if the length of the pipe is not too large (otherwise just subdivide the pipe into a couple of smaller ones). As supposed, this observation can be validated for more involved network structures as well. To confirm this result we have solved the V-net example given in Sect. 4.2 even for the transient model. Figure 8 compares the computed free capacity profiles for the two exits of the V-net obtained for the two models, the quasi-static and the transient one. The shown pictures are very similar to the picture of Fig. 6 that is related to the single pipe.

## Conclusion

We have modeled and numerically solved a time-dependent probabilistic problem for capacity maximization in gas networks with random demand. Two basic models based on transient and quasi-static gas flow, respectively, have been investigated where the latter one is easier to solve and crucial for identifying worst case scenarios. On a simple pipe, both models yielded very similar results for maximum capacities. In order to check potential deviations as a consequence of branching, the same problem was considered for a V-net. Again, the differences were marginal. This suggests, that the time-dependent probabilistic capacity maximization problem could be solved in general under the assumption of quasi-static flow. This observation has the beneficial consequence that, owing to the much easier explicit random constraints, one may afford the consideration of much larger networks of tree-like structure.

**Acknowledgements** This work is supported by the DFG in the Collaborative Research Centre CRC/Transregio 154, Mathematical Modelling, Simulation and Optimization Using the Example of Gas Networks, Projects B04 and C02. In addition, we thank the DFG for the support within MATH+, the Berlin Mathematics Research Center, and, we thank to the support by the FMJH Program Gaspard Monge in opti-

mization and operations research including support to this program by EDF. Moreover, thanks to Maximilian Schade for helpful discussions.

**Author Contributions** The manuscript is prepared by same contribution of all authors. All authors read and approved the final manuscript.

**Funding** Open Access funding enabled and organized by Projekt DEAL. Funding information is given above.

**Data availability** All data provided within the manuscript.

## Declarations

**Conflict of interest** The authors declare that they have no conflict of interest.

**Ethics approval and consent to participate** Not applicable.

**Consent for publication** Not applicable.

**Open Access** This article is licensed under a Creative Commons Attribution 4.0 International License, which permits use, sharing, adaptation, distribution and reproduction in any medium or format, as long as you give appropriate credit to the original author(s) and the source, provide a link to the Creative Commons licence, and indicate if changes were made. The images or other third party material in this article are included in the article's Creative Commons licence, unless indicated otherwise in a credit line to the material. If material is not included in the article's Creative Commons licence and your intended use is not permitted by statutory regulation or exceeds the permitted use, you will need to obtain permission directly from the copyright holder. To view a copy of this licence, visit <http://creativecommons.org/licenses/by/4.0/>.

## References

- Adelhütte D, Aßmann D, González Grandón T, Gugat M, Heitsch H, Henrion R, Liers F, Nitsche S, Schultze R, Stingl M, Wintergerst D (2021) Joint model of probabilistic-robust (proburst) constraints applied to gas network optimization. *Vietnam J Math* 49:1097–1130. <https://doi.org/10.1007/s10013-020-00434-y>
- Aßmann D, Liers F, Stingl M (2019) Decomposable robust two-stage optimization: an application to gas network operations under uncertainty. *Networks* 74:40–61. <https://doi.org/10.1002/net.21871>
- Berthold H, Heitsch H, Henrion R, Schwientek J (2022) On the algorithmic solution of optimization problems subject to probabilistic/robust (proburst) constraints. *Math Methods Oper Res* 96:1–37. <https://doi.org/10.1007/s00186-021-00764-8>
- Charnes A, Cooper W, Symonds G (1958) Cost horizons and certainty equivalents: an approach to stochastic programming of heating oil. *Manag Sci* 4:235–263
- Curtis F, Wächter A, Zavala V (2018) A sequential algorithm for solving nonlinear optimization problems with chance constraints. *SIAM J Optim* 28:930–958. <https://doi.org/10.1137/16M109003X>
- Domschke P, Hiller B, Lang J, Mehrmann V, Morandin R, Tischendorf C (2021) Gas network modeling: an overview. Preprint no. 411, Collaborative Research Center TRR 154. <https://opus4.kobv.de/opus4-trr154/frontdoor/index/index/docId/411>
- Egger H (2018) A robust conservative mixed finite element method for isentropic compressible flow on pipe networks. *SIAM J Sci Comput* 40(1):A108–A129. <https://doi.org/10.1137/16M1094373>
- Egger H, Giesselmann J, Kunkel T, Philippi N (2023) An asymptotic-preserving discretization scheme for gas transport in pipe networks. *IMA J Numer Anal* 43(4):2137–2168. <https://doi.org/10.1093/imanum/drac032>
- Farshbaf-Shaker MH, Gugat M, Heitsch H, Henrion R (2020) Optimal Neumann boundary control of a vibrating string with uncertain initial data and probabilistic terminal constraints. *SIAM J Control Optim* 58:2288–2311. <https://doi.org/10.1137/19M1269944>

- Geletu A, Hoffmann A, Schmidt P, Li P (2020) Chance constrained optimization of elliptic PDE systems with a smoothing convex approximation. *ESAIM Control Optim Calc Var* 26:70. <https://doi.org/10.1051/cocv/2019077>
- González Grandón T, Heitsch H, Henrion R (2017) A joint model of probabilistic/robust constraints for gas transport management in stationary networks. *Comput Manag Sci* 14(3):443–460. <https://doi.org/10.1007/s10287-017-0284-7>
- Göttlich S, Kolb O, Lux K (2021) Chance-constrained optimal inflow control in hyperbolic supply systems with uncertain demand. *Optim Control Appl Methods* 42:566–589. <https://doi.org/10.1002/oca.2689>
- Gotzes C, Heitsch H, Henrion R, Schultz R (2016) On the quantification of nomination feasibility in stationary gas networks with random load. *Math Methods Oper Res* 84:427–457. <https://doi.org/10.1007/s00186-016-0564-y>
- Grimm V, Schewe L, Schmidt M, Zöttl G (2017) A multilevel model of the European entry-exit gas market. *Math Methods Oper Res* 89:223–255. <https://doi.org/10.1007/s00186-018-0647-z>
- Gugat M, Krug R, Martin A (2023) Transient gas pipeline flow: analytical examples, numerical simulation and a comparison to the quasi-static approach. *Optim Eng* 24:425–446. <https://doi.org/10.1007/s11081-021-09690-4>
- Heitsch H (2020) On probabilistic capacity maximization in a stationary gas network. *Optimization* 69:575–604. <https://doi.org/10.1080/02331934.2019.1625353>
- Heitsch H, Strogies N (2019) Consequences of uncertain friction for the transport of natural gas through passive networks of pipelines. In: Hintermüller M, Rodrigues JF (eds) *Topics in applied analysis and optimisation*. Springer, Cham, pp 211–238. [https://doi.org/10.1007/978-3-030-33116-0\\_9](https://doi.org/10.1007/978-3-030-33116-0_9)
- Huck C, Tischendorf C (2017) Transient modeling and simulation of gas pipe networks with characteristic diagram models for compressors. *PAMM* 17(1):707–708. <https://doi.org/10.1002/pamm.201710322>
- Keil R, Müller A, Kumar M, Rao A (2021) Method for solving chance constrained optimal control problems using biased kernel density estimators. *Optim Control Appl Methods* 42:330–354. <https://doi.org/10.1002/oca.2675>
- Koch T, Hiller B, Pfetsch M, Schewe L (eds) (2015) *Evaluating gas network capacities*, vol 21. MOS-SIAM series on optimization. SIAM, Philadelphia. <https://doi.org/10.1137/1.9781611973693>
- Luedtke J, Ahmed S (2008) A sample approximation approach for optimization with probabilistic constraints. *SIAM J Optim* 19:674–699. <https://doi.org/10.1137/070702928>
- Pagnoncelli BK, Ahmed S, Shapiro A (2009) Sample average approximation method for chance constrained programming: theory and applications. *J Optim Theory Appl* 142:399–416. <https://doi.org/10.1007/s10957-009-9523-6>
- Prékopa A (1995) *Stochastic programming*. Kluwer Academic Publishers, Dordrecht
- Schuster M, Strauch E, Gugat M, Lang J (2022) Probabilistic constrained optimization on flow networks. *Optim Eng* 23:1–50. <https://doi.org/10.1007/s11081-021-09619-x>
- Shapiro A, Dentcheva D, Ruszczyński A (2009) *Lectures on stochastic programming*. Model Theory. <https://doi.org/10.1137/1.9780898718751>
- van Ackooij W (2020) A discussion of probability functions and constraints from a variational perspective. *Set-Valued Var Anal* 28:585–609. <https://doi.org/10.1007/s11228-020-00552-2>
- van Ackooij W, Demassez S, Javal P, Morais H, Oliveira W, Swaminathan B (2021) A bundle method for nonsmooth dc programming with application to chance-constrained problems. *Comput Optim Appl* 78:451–490. <https://doi.org/10.1007/s10589-020-00241-8>
- Wang G, Cheng Q, Zhao W, Liao Q, Zhang H (2022) Review on the transport capacity management of oil and gas pipeline network: challenges and opportunities of future pipeline transport. *Energy Strateg Rev* 43:100933. <https://doi.org/10.1016/j.esr.2022.100933>